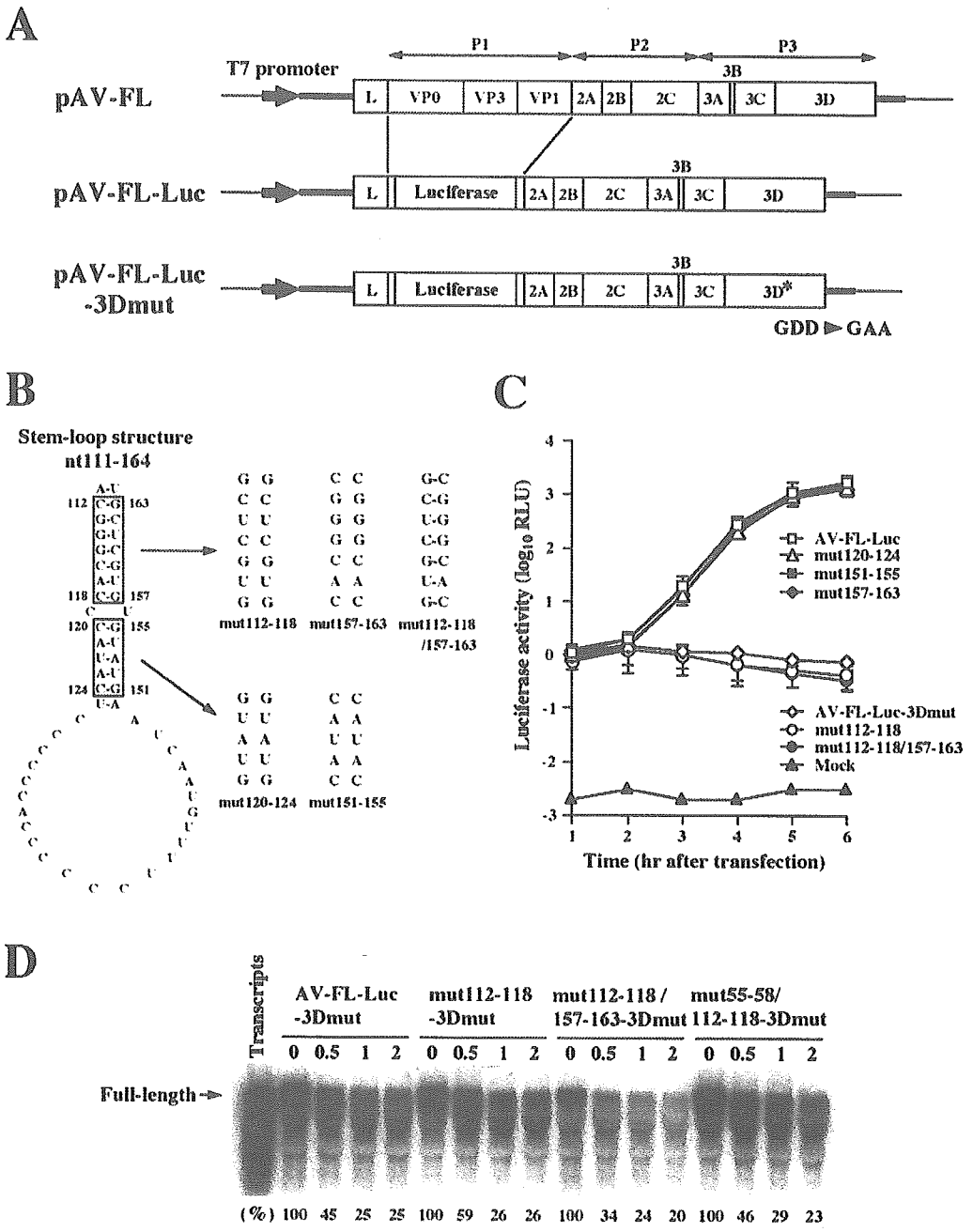

FIG. 2. (A) Organization of the Aichi virus infectious cDNA clone, pAV-FL, and the Aichi virus replicon harboring a luciferase gene, pAV-FL-Luc, and pAV-FL-Luc-3Dmut. The thick lines and open boxes show the untranslated regions and coding regions, respectively. The thin lines indicate the vector sequences. The Aichi virus sequence was cloned just downstream of the T7 promoter sequence. (B) Site-directed mutations introduced into the stem-loop structure (nt 111 to 164) predicted downstream of SL-C. (C) Luciferase activity in cells transfected with AV-FL-Luc and mutants as to the predicted stem-loop structure. Vero cells were electroporated with the RNAs, and then at the indicated times after electroporation, cell lysates were prepared and analyzed for luciferase activity. The experiment was repeated at least three times. Standard deviation bars are shown. (D) RNA stability in Vero cell extracts. ^{32}P-labeled RNA transcripts were incubated at 32°C. At the indicated times after incubation, RNA was extracted, treated with glyoxal, and analyzed by 1% agarose gel electrophoresis. The gel was dried, and radioactive signals were detected with a phosphorimager. Signal intensities of viral RNAs were quantitated, and the percentages of intensities relative to that obtained at 0 h after incubation are shown. Labeled AV-FL-Luc-3Dmut RNA was loaded in the lane represented as input RNA to show its electrophoretic mobility.

segment of SL-B and nt 112 to 115 (CGGG) is critical for viral RNA replication.

Construction of AiV-EMCV chimera replicons. The IRES elements of picornavirus genomes or the hepatitis C virus (HCV) subgenomic replicon can be replaced by the IRES elements of other viruses, and the resulting chimeric viruses have been used to analyze the IRES function and to map the sequences responsible for viral RNA replication without any

TABLE 1. Ability of mutant RNAs to produce viruses

RNA	Virus titer[a] (PFU/ml)	Plaque size[b] (mm)
AV-FL	1.4×10^6	2.1 ± 0.1
mut112-118	0	
mut157-163	1.0×10^6	2.1 ± 0.1
mut112-118/157-163	0	
mut120-124	1.1×10^6	1.7 ± 0.2
mut151-155	1.3×10^6	1.8 ± 0.1
mut55-58/112-118	0	
mut55-60/112-118	3.8×10^4	0.9 ± 0.1
mut57-60/112-118	1.1×10^4	0.9 ± 0.1

[a] Titers of infectious viruses in the cells collected at 72 h after transfection.
[b] Values are the average diameters of 20 plaques ± standard deviations. The sizes were determined at 96 h after transfection.

influence on translation (1, 10, 14, 22, 25, 40). We tried to determine the Aichi virus 5′-end sequence required for RNA replication by using chimera replicons whose 5′ UTRs consist of various lengths of the Aichi virus 5′-terminal sequence and the EMCV IRES (Fig. 4A). We first constructed pAV/EMCV-Luc5′-385. In this construct, the approximately 350 nucleotides (nt 386 to 742) upstream of the translation initiation codon were replaced with the EMCV IRES (Fig. 4A). The IRES element of Aichi virus has not been mapped yet. However, since almost all picornavirus IRESs consist of approximately 450 nucleotides, we thought that the 385 nucleotides of the 5′ end of the Aichi virus genome would include the 5′-terminal part of an IRES, i.e., that the 5′-terminal 385 nucleotides would contain the region required for RNA replication. As a negative control, we constructed pAV/EMCV-Luc5′-385-3Dmut, in which the GDD motif of the 3D RNA-dependent RNA polymerase was changed. Upon in vitro transcription/translation analysis with rabbit reticulocyte lysate, no apparent decrease in the translation efficiency was observed for pAV/EMCV-Luc5′-385 and pAV/EMCV-Luc5′-385-3Dmut compared with that for pAV-FL-Luc (data not shown).

To examine the translation and RNA replication abilities in transfected cells, in vitro transcripts of pAV/EMCV-Luc5′-385 and pAV/EMCV-Luc5′-385-3Dmut were electroporated into Vero cells and then the luciferase activities in the transfected cells were measured (Fig. 4B). At 1 h after transfection, the luciferase activities of AV-FL-Luc and AV-FL-Luc-3Dmut were at almost the same level with each other. This indicates that, at this time, replication of the replicons had hardly occurred and that the luciferase activity in transfected cells represents translation from input RNAs. At 1 h after transfection, AV/EMCV-Luc5′-385 RNA and AV/EMCV-Luc5′-385-3Dmut RNA were slightly lower than those of AV-FL-Luc and AV-FL-Luc-3Dmut in cells transfected with AV/EMCV-Luc5′-385 RNA and AV/EMCV-Luc5′-385-3Dmut RNA, respectively. This indicates that the chimeric replicons had only a slight defect in translation in transfected cells compared to wild-type replicons. At 3 h after transfection, the luciferase activity in the AV/EMCV-Luc5′-385 RNA-transfected cells began to increase. Although the increase in the luciferase activity in the AV/EMCV-Luc5′-385 RNA-transfected cells was slower than that in the AV-FL-Luc RNA-transfected cells, the level at 6 h was similar to that in the case of AV-FL-Luc (Fig. 4B). These results show that AV/EMCV-Luc5′-385 RNA replicates efficiently in transfected cells. We considered that we could map the 5′-terminal sequence of the Aichi virus genome required

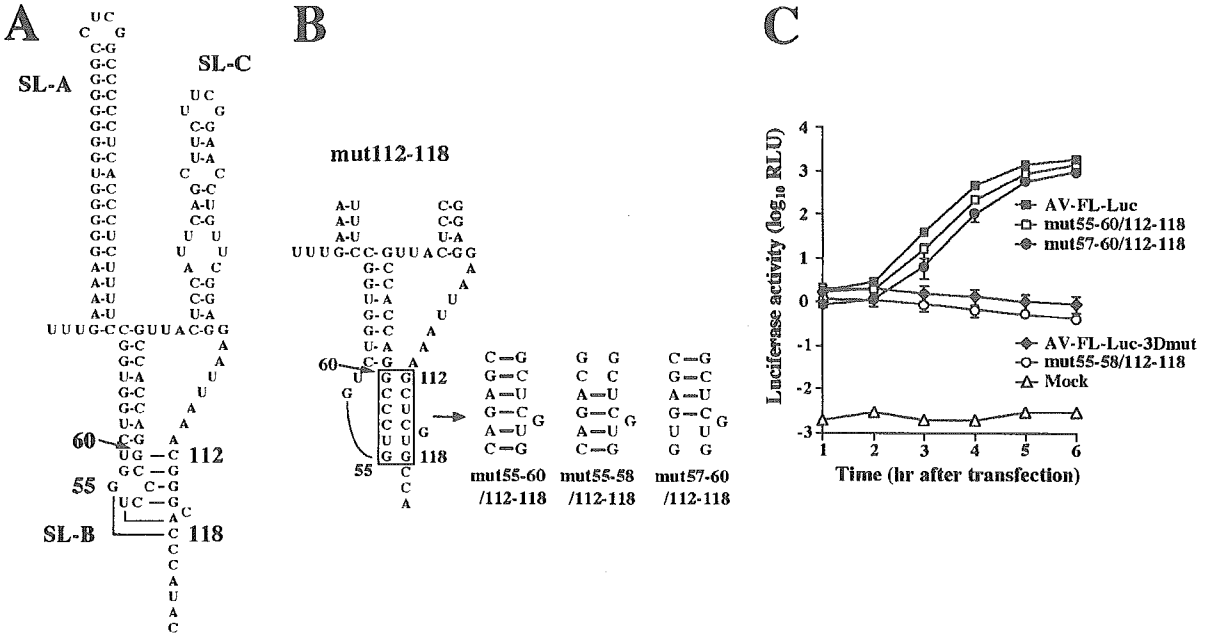

FIG. 3. (A) The predicted pseudoknot structure. Nt 55 to 60 in the loop segment of SL-B can interact with nt 112 to 118, excluding the cytosine at nt 116. (B) Site-directed mutations introduced into mut112-118 to examine the base-pairing interactions. (C) Luciferase activity in cells transfected with AV-FL-Luc and mutants as to the predicted pseudoknot structure. Vero cells were electroporated with RNAs, and then at the indicated times after electroporation, cell lysates were prepared and analyzed for luciferase activity. The experiment was repeated at least three times. Standard deviation bars are shown.

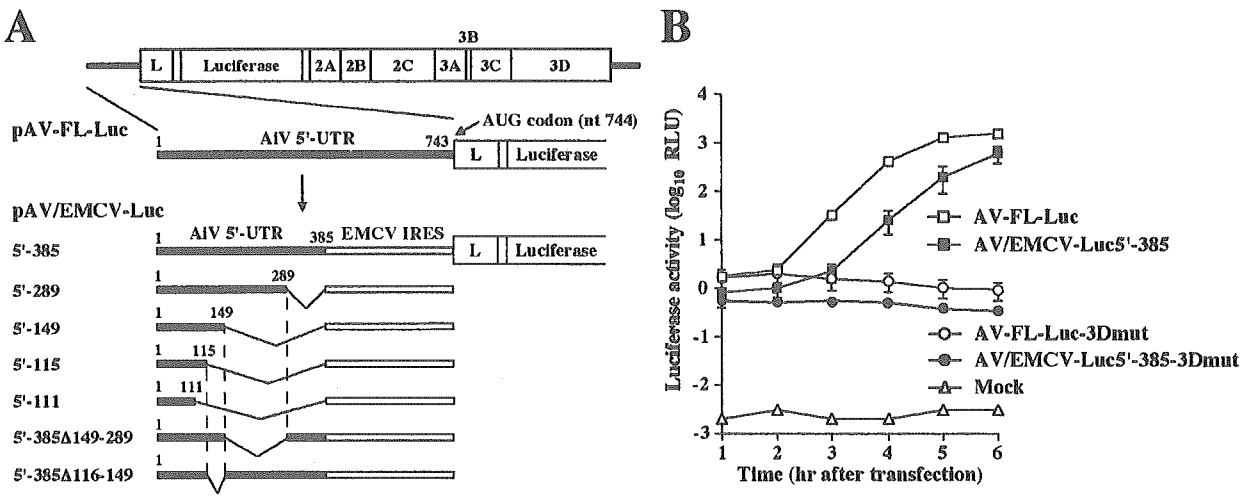

FIG. 4. (A) Schematic diagram of the 5′ UTR of Aichi virus and chimera replicons. The thick lines indicate the Aichi virus sequences in the 5′ UTR. Each plasmid name shows the number of Aichi virus nucleotides retained at the 5′ end. The open boxes indicate EMCV IRES. (B) Luciferase activity in the transfected cells with AV-FL-Luc, AV/EMCV-Luc5′-385, AV-FL-Luc-3Dmut, and AV/EMCV-Luc5′-385-3Dmut. Vero cells were electroporated with the RNAs, and then at the indicated times after electroporation, cell lysates were prepared and analyzed for luciferase activity. The experiment was repeated at least three times. Standard deviation bars are shown.

for RNA replication using this chimera replicon without any influence on translation.

Mapping of the essential element for viral RNA replication. We investigated the 5′-end sequence required for RNA replication by using AV/EMCV-Luc5′-385 and a series of deletion mutants (AV/EMCV-Luc5′-289, AV/EMCV-Luc5′-149, AV/EMCV-Luc5′-115, and AV/EMCV-Luc5′-111) (Fig. 4A).

The replicon with the 5′-end 111 nucleotides of Aichi virus at the 5′ end (AV/EMCV-Luc5′-111), which does not include the pseudoknot structure, could not replicate (Fig. 5A). This replicon appeared to have a slight defect in the translation activity, as indicated by the luciferase activity at 1 h after transfection; however, its activity was significantly higher than that in mock-transfected cells. No significant decrease in RNA stability was observed for AV/EMCV-Luc5′-111-3Dmut compared with that for AV-FL-Luc-3Dmut and AV/EMCV-Luc5′-385-3Dmut (Fig. 5B). The inability of AV/EMCV-Luc5′-111 to replicate would be due mainly to disruption of the pseudoknot structure. In contrast, replication of the replicon carrying the 5′-end 115 nucleotides of Aichi virus at the 5′ end (AV/EMCV-Luc5′-115), in which the pseudoknot structure could be formed, was observed. The mutants with the longer Aichi virus 5′-terminal sequences at the 5′ end (AV/EMCV-Luc5′-149 and AV/EMCV-Luc5′-289) replicated more efficiently (Fig. 5A). These results indicate that the 5′-end 115 nucleotides of the genome including the pseudoknot structure are the minimum requirement for RNA replication. In addition, these results also imply that a sequence downstream of the pseudoknot structure participates in enhancement of the RNA replication efficiency.

Then, to determine whether any element enhancing the replication efficiency was present in the sequence downstream from nt 115, deletions of nt 116 to 149 and nt 149 to 289 were introduced into pAV/EMCV-Luc5′-385, yielding pAV/EMCV-Luc5′-385Δ116-149 and pAV/ENCV-Luc5′-385Δ149-289, respectively (Fig. 4A). The luciferase assay showed that the deletion of nt 149 to 289 had only a modest effect on the RNA replication efficiency (Fig. 5C). The deletion of nt 116 to 149 also did not severely affect the efficiency of replication. These results, together with the finding that the deletion of nt 289 to 385 had a modest effect on replication (AV/EMCV-Luc5′-289) (Fig. 5A), suggest that the presence of the sequence downstream of the pseudoknot structure enhances the RNA replication efficiency but that a region absolutely required for enhancement might not exist.

Cell-free replication system for Aichi virus. The cell-free translation/replication system was first developed for poliovirus by Molla et al. (29), and since then, this system has been frequently used as a powerful tool for analyzing the mechanism of poliovirus replication. In this study, we tried to develop a cell-free translation/replication system for Aichi virus.

(i) A *cis*-active hammerhead ribozyme. It has been reported that efficient replication of poliovirus RNA in HeLa cell extracts requires a precise 5′ end and that a *cis*-active hammerhead ribozyme is used to remove the nonviral nucleotides present at the 5′ ends of T7 RNA polymerase-synthesized transcripts derived from a poliovirus full-length cDNA clone (19). We performed mutagenesis to introduce a *cis*-active hammerhead ribozyme at the 5′ end of the Aichi virus cDNA sequence using a plasmid, pU5′Eco (42), which contained the T7 promoter and the 5′-end 391 nucleotides of the Aichi virus genome. First, we constructed a hammerhead ribozyme whose stem I comprised 8 base pairs (pU5′Eco-5′rzm-8bp) (Fig. 6A). pU5′Eco linearized by digestion with HindIII would give rise to RNA 444 nt in length upon in vitro transcription with T7 RNA polymerase, and, on the other hand, transcripts derived from pU5′Eco-5′rzm-8bp would be 505 nt in length before cleavage. When transcripts synthesized from pU5′Eco-5′rzm-8bp were electrophoresed on a denaturing polyacrylamide gel, two products were detected, the shorter one being the same size as the transcripts synthesized from pU5′Eco (Fig. 6B, lanes 1 and 2). This shorter product, which is thought to be the

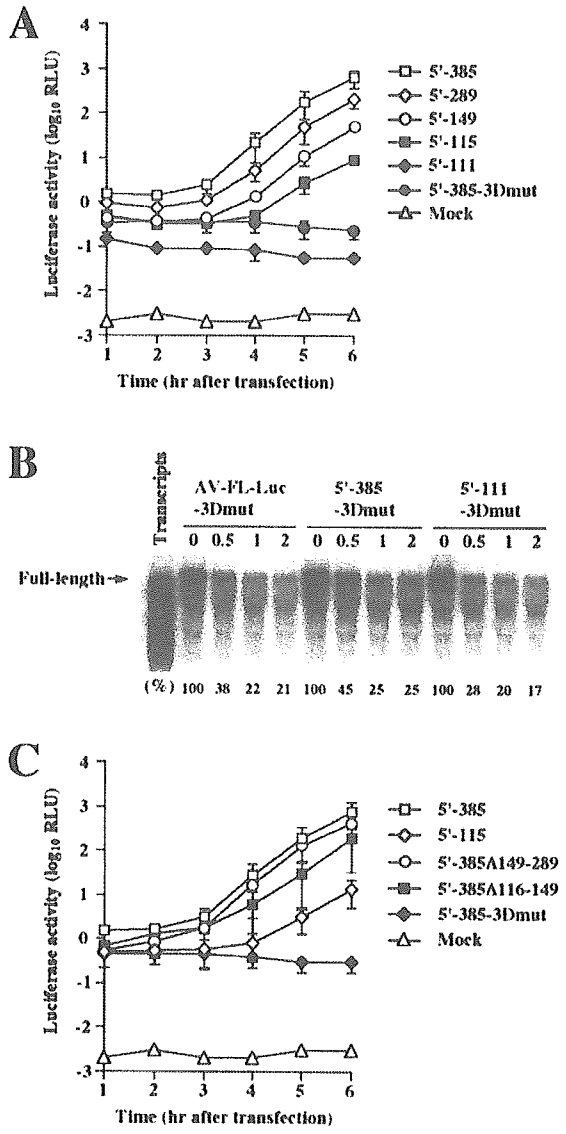

FIG. 5. (A and C) Luciferase activity in cells transfected with AV/EMCV-Luc5′-385 and a series of deletion mutants as to the 5′ UTR. Vero cells were electroporated with the RNAs, and then at the indicated times after electroporation, cell lysates were prepared and analyzed for luciferase activity. The experiment was repeated at least three times. Standard deviation bars are shown. (B) RNA stability of AV-FL-Luc-3Dmut RNA, AV/EMCV-Luc5′-385-3Dmut RNA, and AV/EMCV-Luc5′-111-3Dmut RNA in Vero cell extracts. RNA stability was analyzed as described in the legend to Fig. 2D. Signal intensities of viral RNAs were quantitated, and the percentages of intensities relative to that obtained at 0 h after incubation are shown.

cleaved form, comprised only a small portion of the transcripts. We presumed that the formation of a stable stem-loop structure (SL-A) at the 5′ end of the genome (42) may inhibit the formation of stem I of the hammerhead ribozyme, resulting in inefficient cleavage. Next, we constructed a hammerhead ribozyme with stem I comprising 22 base pairs (pU5′Eco-5′rzm) (Fig. 6A). Transcripts derived from pU5′Eco-5′rzm also contained the uncleaved form (Fig. 6B, lane 3), but the hammerhead ribozyme functioned more efficiently than that in the transcripts derived from pU5′Eco-5′rzm-8bp. We used this hammerhead ribozyme with stem I comprising 22 base pairs in the following experiments.

(ii) Virus production in Vero cell S10 extracts. For the cell-free Aichi virus replication system, we used Vero cell S10 extracts. An Aichi virus cDNA clone with the 5′ hammerhead ribozyme sequence, pAV-FL-5′rzm, was constructed (Fig. 6C). To optimize the concentrations of K^+ and Mg^{2+} in cell-free reactions, transcripts synthesized from pAV-FL-5′rzm were incubated in the cell-free reaction mixtures containing various concentrations of K^+ and Mg^{2+} at 32°C for 15 h and then the virus yield was determined by plaque assay. As a result, optimal concentrations of K^+ and Mg^{2+} were determined to be 150 mM and 1.5 mM, respectively, and the virus yield was 3×10^4 PFU/ml. Under these conditions, the reaction programmed with the virion RNA produced viable viruses at the titer of 3×10^5 PFU/ml. This titer is 10-fold higher than that for the reaction programmed with AV-FL-5′rzm RNA. The decreased virus production observed for the reaction programmed with AV-FL-5′rzm RNA was probably due mainly to the incomplete cleavage by the 5′ hammerhead ribozyme. There was no morphological difference between the plaques formed by viruses derived from virion RNA and AV-FL-5′rzm RNA (data not shown). A 25-μl reaction mixture programmed with AV-FL RNA produced no viable viruses.

(iii) Translation and replication of Aichi virus RNA in cell extracts. Reactions were programmed with AV-FL-5′rzm RNA, AV-FL RNA, or AV-FL-3Dmut RNA. AV-FL RNA and AV-FL-3Dmut RNA have three nonviral nucleotides, GGU, at their 5′ ends (Fig. 6C). Translation products of the three RNAs were labeled by adding [^{35}S]methionine-cysteine into the cell-free reaction mixture. Translation of these three RNAs occurred with similar efficiency (Fig. 6D). For detection of RNA synthesized in cell-free reactions, [^{32}P]CTP was added to the reaction mixture at 3 h after the start of the reaction and then the mixture was incubated for an additional 2 h. Product RNAs with or without RNase A and RNase T_1 treatment were analyzed by nondenaturing agarose gel electrophoresis (Fig. 6E). The reaction with AV-FL-5′rzm RNA produced both RNase A/T_1-resistant double-stranded replicative form (RF) and RNase A/T_1-sensitive single-stranded RNA (ssRNA) (lanes 1 and 4). The labeled RF consists of unlabeled inputted positive-strand RNA and labeled negative-strand RNA, while the labeled ssRNA consists of newly synthesized positive-strand RNA (19, 20). When AV-FL RNA was used for a reaction, RF and ssRNA were also detected (lanes 2 and 5); however, the amount of ssRNA was much less than that in the reaction with AV-FL-5′rzm RNA whereas the amounts of RF were similar. This indicates that the extra 3 nucleotides at the 5′ end of the transcript do not affect negative-strand RNA synthesis but significantly impair positive-strand synthesis.

It has been reported that a cell-free reaction programmed with poliovirus RNA with two nonviral guanosine residues at the 5′ end does not produce a detectable level of positive-strand RNA (6, 19). In contrast, in our cell-free system, extra nucleotides at the 5′ end of the transcript appeared not to abolish positive-strand synthesis completely. To further confirm that the reaction programmed with AV-FL RNA produces a detectable amount of positive-strand RNA, RPA was performed with unlabeled probes. For the detection of nega-

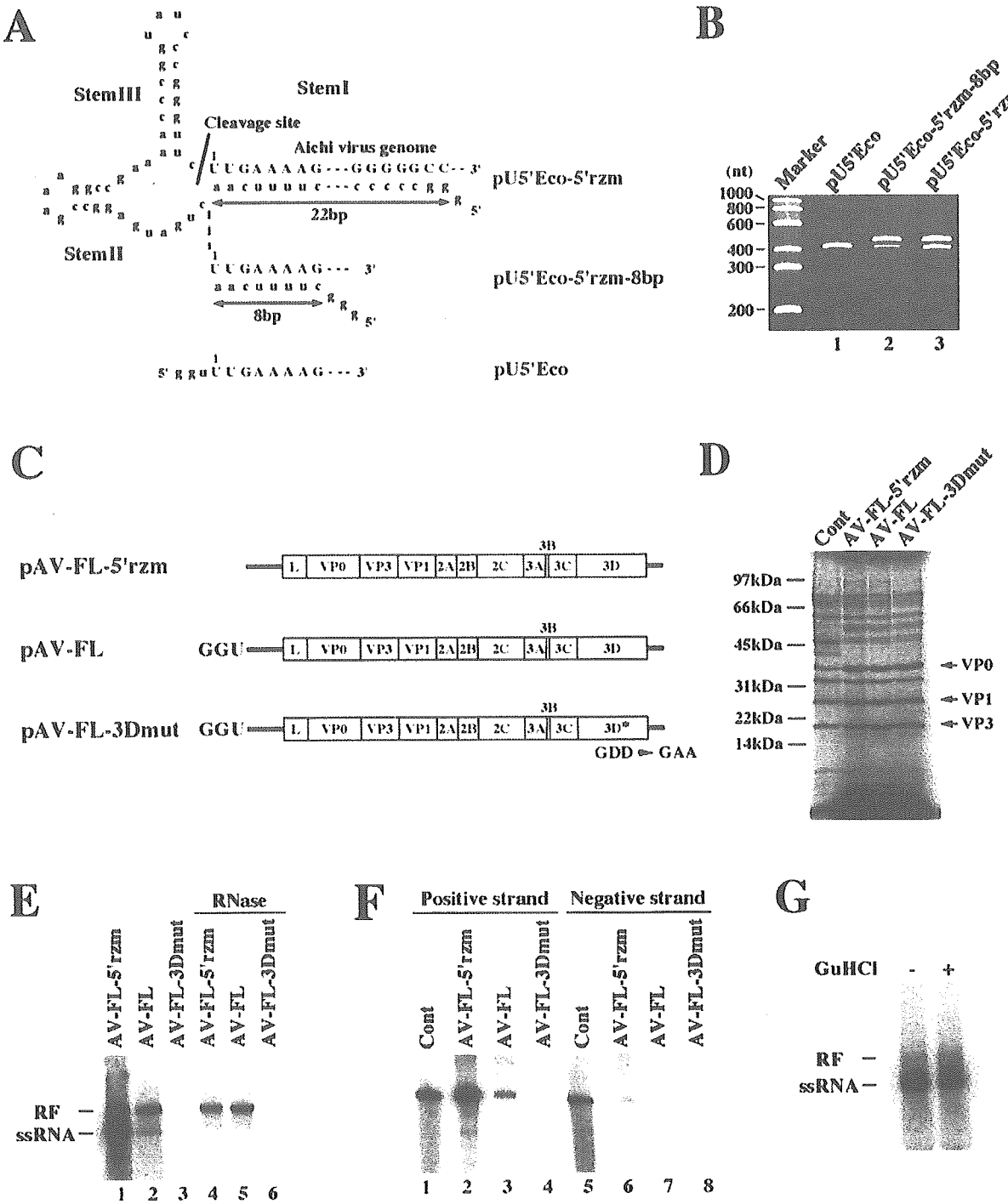

FIG. 6. (A) The 5′ end sequences of in vitro transcripts synthesized from pU5′Eco-5′rzm, pU5′Eco-5′rzm-8bp, and pU5′Eco. pU5′Eco have the T7 promoter followed by the 5′-end 391 nucleotides of the Aichi virus sequence. pU5′Eco-5′rzm and pU5′Eco-5′rzm-8bp were constructed by introducing the *cis*-active hammerhead ribozyme sequence between the T7 promoter and the virus sequence. In pU5′Eco-5′rzm and pU5′Eco-5′rzm-8bp, stem I segments of the ribozyme were 22 bp and 8 bp in length, respectively. The Aichi virus sequences and nonviral nucleotides are represented by uppercase letters and lowercase letters, respectively. (B) Cleavage by the hammerhead ribozyme. In vitro transcripts synthesized from pU5′Eco-5′rzm, pU5′Eco-5′rzm-8bp, and pU5′Eco were electrophoresed on a 3.5% polyacrylamide–7 M urea gel, and then the gel was stained with ethidium bromide. (C) Schematic diagrams of in vitro transcripts derived from full-length cDNA clones. The in vitro transcripts synthesized from plasmids containing the hammerhead ribozyme have a precise 5′ end, while those from plasmids without the hammerhead ribozyme have three nonviral nucleotides, GGU, at the 5′ end. In pAV-FL-3Dmut, the GDD motif within the 3D RNA polymerase-coding sequence was changed to Gly-Ala-Ala to inactivate the RNA polymerase. (D) Protein synthesis in a cell-free reaction programmed with AV-FL-5′rzm RNA, AV-FL RNA, or AV-FL-3Dmut RNA. Reactions were performed in the presence of [^{35}S]methionine-cysteine for 4 h, and then proteins were analyzed by SDS-polyacrylamide gel electrophoresis. In lane represented as Cont, viral proteins that were metabolically labeled with [^{35}S]methionine-cysteine in transfected cells were loaded. The positions of capsid proteins are indicated. (E) RNA products in a cell-free

tive-strand RNA, two-cycle RPA (35) was carried out. AV-FL RNA and AV-FL-5′rzm RNA produced similar amounts of negative-strand RNA (Fig. 6F, lanes 6 and 7). In addition, consistent with the results described above, positive-strand RNA was detected in a much lower amount in the reaction programmed with AV-FL RNA than in that with AV-FL-5′rzm (lanes 2 and 3). Thus, the extra 3 nucleotides at the 5′ ends of Aichi virus RNA transcripts remarkably impaired positive-strand RNA synthesis in our cell-free replication system but synthesized positive-strand RNA was detectable.

(iv) Effect of guanidine hydrochloride (HCl) on Aichi virus RNA replication. It is known that guanidine HCl is an inhibitor of poliovirus RNA replication. Indeed, we confirmed that Vero cells infected with poliovirus exhibited no cytopathic effect in the presence of 2 mM of guanidine HCl (data not shown). In contrast, addition of 2 mM of guanidine HCl to the cell culture medium did not inhibit Aichi virus replication. AV-FL-Luc RNA replicated in transfected cells in the presence of 2 mM of guanidine HCl as efficiently as in the absence of guanidine HCl (data not shown). In addition, in cell extracts, the presence of 2 mM of guanidine HCl did not affect the replication of AV-FL-5′rzm RNA (Fig. 6G). Thus, guanidine HCl is not an inhibitor of Aichi virus RNA replication.

In most studies on poliovirus using the cell-free system, preinitiation replication complexes isolated from the cell-free reaction containing 2 mM guanidine HCl (4) are used for analyzing RNA replication. In the following experiments of this study, however, analyses of RNA synthesis in cell extracts were performed without isolating preinitiation replication complexes, due to the insensitivity of Aichi virus to guanidine HCl.

In summary, a cell-free translation/replication system for Aichi virus was established and it became possible to analyze the replication of genetically engineered Aichi virus RNAs in cell extracts by using transcripts synthesized from a *cis*-active hammerhead ribozyme-containing full-length cDNA clone.

The 5′ end of the Aichi virus genome is important for both positive- and negative-strand RNA synthesis. We have already carried out site-directed mutational analysis of the 5′ end of the genome and obtained many mutants that could not replicate in transfected cells (33, 42). In this study, using cell extracts that can support the translation, replication, and encapsidation of Aichi virus RNA, we investigated the abilities of these mutants to synthesize positive- and negative-strand RNAs. mut5, mut9, mutB-1, mutB-4, mutC-7, and mut112-118 were used for this experiment (Fig. 7). mut5 contains a 7-nucleotide mutation (nt 32 to 38) in the middle part of the stem of SL-A to disrupt the base-pairings of the stem, and mut9 was constructed by exchanging 6-nucleotide stretches (nt 3 to 8 and 39 to 44) in the lower part of the stem of SL-A with each other to maintain the base-pairings of the stem of SL-A (42). mutB-1 and mutC-7 contain mutations that disrupt the base-pairings of the stem of SL-B and the lower stem of SL-C, respectively (33). In mutB-4, which has nucleotide changes in the loop region of SL-B (33), and mut112-118, the formation of the pseudoknot structure was prevented (Fig. 3B). Upon dot blot hybridization or luciferase assay, replication of these mutants was not observed in transfected cells (33, 42) (Fig. 2C).

First, translation of mutant RNAs in Vero cell extracts was examined. In this system, newly synthesized proteins can be detected independent of RNA replication. No significant differences in the translation efficiency among these mutants were observed (Fig. 8A).

Next, RNA synthesis of the mutants in a cell-free reaction was investigated. In the analysis using RNAs that have three nonviral nucleotides (GGU) at the 5′ end (Fig. 6C), no RF band was detected for the reaction programmed with mut5 (Fig. 8B, lane 3). mutB-1, mutB-4, and mutC-7 produced only faint bands (lanes 5 to 7). mut112-118 synthesized RF and positive-strand RNA at significantly lower levels than those for AV-FL, although the ratio of positive-strand RNA to RF was similar for AV-FL and mut112-118. These results indicate that mut5, mutB-1, mutB-4, mutC-7, and mut112-118 have a defect in negative-strand synthesis. In contrast, mut9 generated only an RF band, i.e., ssRNA was not detected (Fig. 8B, lane 4), indicating that mut9 has a defect in positive-strand synthesis but not in negative-strand synthesis.

The abilities of mut112-118 and mut9 to produce positive-strand RNA were further investigated using mut112-118-5′rzm RNA and mut9-5′rzm RNA. The hammerhead ribozymes introduced into these two mutants exhibited a similar level of the cleavage efficiency compared to that introduced into AV-FL-5′rzm (Fig. 8C). As expected, mut112-118-5′rzm generated positive-strand RNA more efficiently than mut112-118 (Fig. 8D, compare lanes 5 and 6). mut112-118-5′rzm and mut112-118 produced smaller amounts of positive-strand RNA and RF than AV-FL-5′rzm and AV-FL, respectively. Quantitative analysis showed that the amount of the RF synthesized by mut112-118 was sevenfold less than that synthesized by AV-FL and that the amount of ssRNA produced by mut112-118 to 5′rzm was sixfold less than that in AV-FL-5′rzm (Fig. 8D). However, the ratio of positive-strand RNA to RF was similar between the two RNAs (compare lanes 1 and 5). This further indicates that mut112-118 has a defect in negative-strand synthesis, not in positive-strand synthesis. In contrast, mut9-5′rzm synthesized no detectable level of ssRNA, indicating a defect of this mutant in positive-strand RNA synthesis.

Overall, the results of analysis of RNA synthesis by the mutants using the cell-free replication system indicate that the formation of the proper secondary and tertiary structures at

---

reaction programmed with AV-FL-5′rzm RNA, AV-FL RNA, or AV-FL-3Dmut RNA. RNA was labeled with [α-^{32}P]CTP at 3 to 5 h after the start of incubation, and then total RNA was extracted. The extracted RNA was analyzed by nondenaturing agarose gel electrophoresis after being either treated with RNase A and RNase T_1 (lanes 4 to 6) or untreated (lanes 1 to 3). The positions of double-stranded RF and ssRNA are indicated. (F) RPA. Labeled viral RNA products of a cell-free reaction were subjected to RPA using an unlabeled probe that hybridizes with the Aichi virus positive-strand RNA or negative-strand RNA. To detect the negative-strand RNA, two-cycle RPA was carried out. As a positive control (Cont), in vitro-labeled full-length positive-strand or negative-strand RNA was used. Protected RNAs were analyzed by 3.5% polyacrylamide–7 M urea gel electrophoresis. (G) Effect of guanidine HCl on viral RNA replication in cell extracts. AV-FL-Luc-5′rzm RNA was used for a cell-free reaction with or without 2 mM guanidine HCl. Labeled RNA products were analyzed by nondenaturing agarose gel electrophoresis. The positions of RF and ssRNA are indicated.

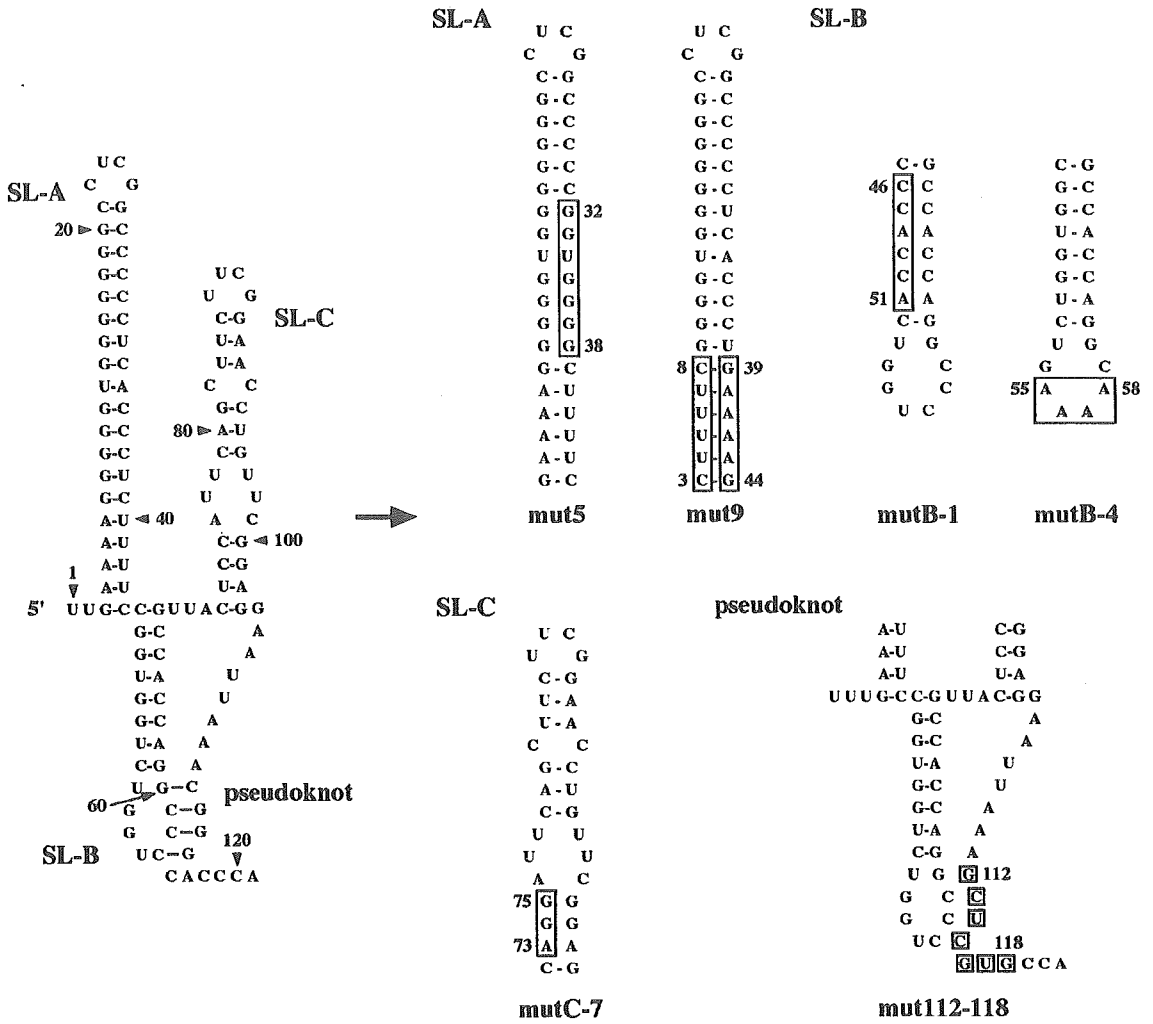

FIG. 7. Site-directed mutations introduced into the three stem-loop and pseudoknot structures. The mutated regions and nucleotides are boxed.

the 5′ end of the genome is required for negative-strand RNA synthesis. In addition, it was shown that mutations of the primary sequence in the lower part of the stem of SL-A abolishes positive-strand RNA synthesis.

DISCUSSION

Computer-assisted secondary structure prediction suggested the formation of a stem-loop structure at nt 111 to 164, besides the previously defined three stem-loop structures SL-A, SL-B, and SL-C (Fig. 1). In this study, using various site-directed mutants, we examined whether the predicted stem-loop structure downstream of SL-C is important for virus replication. As a result, folding of this stem-loop structure (nt 111 to 164) was found to not be important for RNA replication (Fig. 2), but a novel structural element, a pseudoknot structure, was detected. This pseudoknot structure is formed through interaction between nt 57 to 60 in the loop segment of SL-B and nt 112 to 115, and its proper folding is critical for RNA replication (Fig. 3). The formation of a pseudoknot structure is predicted at the 5′ ends of the genomes of other picornaviruses including cardio-, parecho-, and hepatoviruses (11, 13, 17, 24), and, for mengovirus and human parechovirus 1, experimental data showing the importance of pseudoknot structures for RNA replication have been presented (27, 34). Recently, a virus, the U-1 strain, related to Aichi virus was discovered and its complete genome sequence was determined (49). The 5′-terminal region of the genome of strain U-1 is predicted to fold into three stem-loop structures similar to those in Aichi virus (49). We found that the 5′-terminal region of strain U-1 has the potential to form a pseudoknot structure similar to that found in Aichi virus (data not shown).

This study also indicated that the 5′-end 115 nucleotides including the pseudoknot are the minimum requirement for RNA replication. The chimera replicon harboring the 5′-terminal 111 nucleotides of the genome (AV/EMCV-Luc5′-111), which does not include the pseudoknot structure, did not replicate (Fig. 5A). In contrast, replication of AV/EMCV-Luc5′-115, in which the pseudoknot structure is formed, was observed. However, the chimera replicons harboring the longer 5′-terminal sequences of the Aichi virus genome replicated

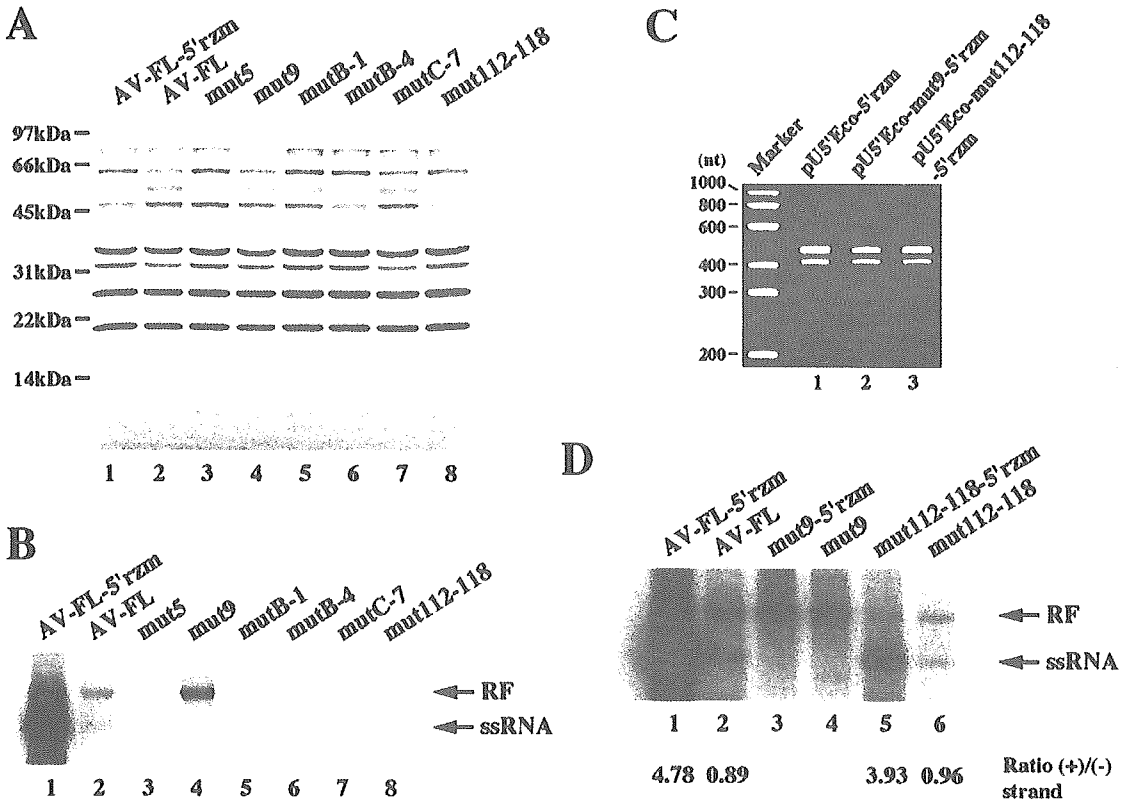

FIG. 8. (A) Translation of mutant RNAs in Vero cell extracts. RNA transcripts were subjected to in vitro translation reaction in the presence of [^{35}S]methionine-cysteine for 4 h at 32°C. The translation products were electrophoresed on an SDS-polyacrylamide gel, and then the gel was dried. Radioactive signals were detected with a phosphorimager. (B) Positive- and negative-strand RNA synthesis in the cell-free reactions. The product RNA was analyzed by native agarose gel electrophoresis. Radioactive signals were detected with a phosphorimager. The positions of RF and ssRNA are indicated. (C) Cleavage by the hammerhead ribozyme. In vitro transcripts synthesized from pU5′Eco-5′rzm, pU5′Eco-mut9-5′rzm, and pU5′Eco-112-118-5′rzm were electrophoresed on a 3.5% polyacrylamide–7 M urea gel, and then the gel was stained with ethidium bromide. (D) Positive- and negative-strand RNA synthesis in cell-free reactions of mut9 and mut112-118 harboring the 5′ hammerhead ribozyme. The ratios of positive-strand to negative-strand RNA synthesis are indicated.

more efficiently (Fig. 4A and 5A). It has been reported that stem-loop II within the poliovirus IRES is involved in RNA replication (21, 45). In HAV, the 5′-end 94 nucleotides of the genome fold into stem-loop structures with the potential to form pseudoknot structures (11, 44); however, an experiment involving chimera replicons showed that the 5′-end 237 nucleotides are required for RNA replication (22). Since the 5′ border of the HAV IRES is mapped between nt 151 and 257 (10), the 5′-end 237 nucleotides may contain the 5′ part of the IRES. In addition, it has been shown in HAV that the nucleotide sequence of bases 140 to 144 is essential for efficient replication in cultured cells (44). In the case of Aichi virus, deletion of either nt 116 to 149, 149 to 289, or 289 to 385 did not severely decrease the RNA replication efficiency compared to that in the case of AV/EMCV-Luc5′-385 (Fig. 5A and C). Thus, there appears to be no region absolutely necessary for enhancement of the replication efficiency.

It is possible that the nucleotide sequence downstream of nt 115 serves to spatially separate the two elements, i.e., the 5′-terminal *cis*-acting replication element and the IRES, or to allow the two elements to fold into the proper structures. In the HCV replicon harboring the poliovirus IRES, when the HCV 5′ UTR is directly fused to the poliovirus IRES, the poliovirus IRES activity is severely impaired (14). The introduction of a spacer element between the HCV 5′ UTR and the poliovirus IRES of the replicon improves the translation activity. Also, in this study, the translation activity of AV/EMCV-Luc5′-111 was found to be reduced (Fig. 5A). Although a significant reduction in the translation activity of the other chimera replicons with reduced RNA replication ability was not observed, it is possible that the proper folding of the 5′-end *cis*-element or -binding of proteins required for RNA replication to the 5′-end *cis*-element is prevented. Very recently, it was shown that the poliovirus RNA with the complete IRES deletion replicates in cell-free translation-replication reactions (32). A similar approach will clarify further the role of the nucleotide sequence downstream of nt 115 in RNA replication. In addition, this approach will also help to exclude the possibility that the EMCV IRES introduced into chimera replicons contains sequences that affect Aichi virus RNA replication.

In this study, we established a cell-free replication system for Aichi virus. Vero S10 extracts programmed with in vitro transcripts synthesized from a full-length cDNA clone containing a *cis*-active hammerhead ribozyme generated viable viruses. Thus, it became possible to analyze Aichi virus replication in cell extracts using genetically engineered viral RNA.

The cell-free replication system has been used as a powerful tool to analyze the mechanism of poliovirus RNA replication, because using this system, it is possible to distinguish between mutant RNAs defective in the synthesis of negative- and positive-strand RNA. Our system also made this possible. By electrophoresis of the product RNAs of cell-free reactions on a nondenaturing agarose gel, labeled double-stranded RF and ssRNA were detected. Labeled RF and ssRNA are indications of the synthesis of negative-strand RNA and positive-strand RNA, respectively (19, 20).

As reported for poliovirus (19), removal of extra nucleotides at the 5′ end of the genome using a hammerhead ribozyme resulted in a significant increase of positive-strand synthesis in a cell-free reaction (Fig. 8D, compare lanes 1 and 2). However, the *cis*-active hammerhead ribozyme that we designed did not function completely (Fig. 6B, lane 3). A subset of AV-FL-5′rzm RNA, which still has the uncleaved ribozyme sequence at the 5′ end, would function as a template for the negative-strand RNA. But the negative-strand RNAs complementary to the sequence of the uncleaved ribozyme sequence at the 3′ end would not serve as templates for positive-strand synthesis. This would be a cause of the relatively low value of the ratio of ssRNA to RF (5:1) observed in a cell-free reaction of AV-FL-5′rzm RNA (Fig. 8D) compared to the ratio reported in a cell-free reaction of poliovirus (20:1) (19). It is necessary to enhance the cleavage efficiency of the ribozyme for a detailed quantitative analysis of positive-strand synthesis. On the other hand, for a quantitative analysis of negative-strand synthesis, RNA with extra nucleotides at the 5′ end would be more suitable than RNA synthesized from the plasmid harboring the 5′ ribozyme because the RF synthesized by RNA with the accurate 5′ end is used efficiently as a template for positive-strand synthesis, resulting in the conversion of the RF to replicative intermediate RNA.

Using cell extracts, we investigated the replication properties of mutants harboring a lethal mutation in the 5′-terminal region. Mutations disrupting structural elements abolished or impaired negative-strand RNA synthesis remarkably. mut112-118, in which formation of the pseudoknot structure is prevented, produced very small amounts of positive- and negative-strand RNAs in the cell-free reaction. Interestingly, the ratio of positive-strand RNA to RF was similar for AV-FL-5′rzm and mut112-118-5′rzm (Fig. 8D, lanes 1 and 5). Since the ribozymes in the two RNAs exhibited a cleavage efficiency similar to each other (Fig. 8C, lanes 1 and 3), this result implies that the two RNAs synthesize positive-strand RNA with an equivalent efficiency. That is, this suggests that disruption of the pseudoknot structure affects negative-strand RNA synthesis but not positive-strand RNA synthesis. On the other hand, nucleotide changes in the lower part (nt 3 to 8/39 to 44) of the stem of SL-A to maintain the base-pairings of the stem did not affect negative-strand synthesis but abolished positive-strand RNA synthesis (Fig. 8D, mut9).

In poliovirus, the 5′ cloverleaf structure binds to 3CD and PCBP (2, 3, 16, 36) and 3CD and PCBP interact with poly(A)-binding protein that binds to the poly(A) tract at the 3′ end of the genome (7, 20, 26). Such genome circularization is required for negative-strand RNA synthesis. It is likely that the 5′-terminal structural elements of the Aichi virus genome function in a similar manner in negative-strand synthesis. Disruption of the 5′-terminal structural elements would probably prevent interaction with proteins required for genome circularization. We intend to identify viral or host proteins interacting with the 5′-terminal structural elements of the Aichi virus genome.

Also, the involvement of the poliovirus 5′ cloverleaf structure in positive-strand synthesis has previously been reported (2). Mutation of stem-loop b or d, which affects formation of the RNP complex, reduced the ratio of positive- to negative-strand RNA accumulated in infected cells (2). However, it has also been shown that the same mutation introduced into stem-loop d inhibits negative-strand RNA synthesis severely in the cell-free reaction (7). In this study, we demonstrated clearly that a mutation in the 5′-end nucleotide sequence (mut9) abolishes positive-strand RNA synthesis without affecting negative-strand synthesis using the cell-free translation-replication system (Fig. 8D, lanes 3 and 4). For Sindbis virus, it has been reported that the 5′ end of the genome contains *cis*-acting elements that regulate minus- and plus-strand RNA synthesis. A notable finding is that deletion of the very 5′-end nucleotides (nt 2 to 4 or nt 5) had no or only a moderate effect on minus-strand RNA synthesis but almost completely abolished plus-strand synthesis (15).

It is possible that the 5′-end sequence functions in the complementary sequence, i.e., in the 3′ end of the negative-strand RNA, for positive-strand synthesis. It should be noted that, in mut9, the nucleotide change was introduced into the sequence that serves as the template for the addition of nucleotides directly to VPgpUpU, which is the primer for positive-strand RNA synthesis (18, 30, 31). The specific 3′-end nucleotide sequence of the negative-strand RNA may be required for direct binding with 3D polymerase or for promotion of the assembly of a complex required for the initiation of positive-strand RNA synthesis. Recently, it has been shown that the 3′ UTR of the poliovirus genome is involved in positive-strand RNA synthesis (9). This suggests that the 5′-end region of the negative-strand RNA, which is the complementary sequence to the 3′ UTR, interacts with the 3′ end of the negative-strand RNA to initiate positive-strand RNA synthesis. The 3′-end nucleotide sequence of the negative-strand RNA may interact with the viral or cellular proteins required to circularize the negative-strand RNA. Further experiments are required to determine the role of the 5′-end sequence in positive-strand RNA synthesis.

In conclusion, this study has indicated that the 5′-end 115 nucleotides of the Aichi virus genome are the minimum requirement for viral RNA replication and that they encode elements required for positive- and negative-strand RNA synthesis. It has been previously shown that the most 5′-end stem-loop structure, SL-A, is involved in RNA encapsidation. Thus, the 5′ terminus of the Aichi virus genome is a multifunctional region.

ACKNOWLEDGMENT

This work was supported in part by a Grant-in-Aid for Scientific Research from the Ministry of Education, Culture, Sports, Science and Technology of Japan.

REFERENCES

1. **Alexander, L., H. H. Lu, and E. Wimmer.** 1994. Polioviruses containing picornavirus type 1 and/or type 2 internal ribosomal entry site elements:

genetic hybrids and the expression of a foreign gene. Proc. Natl. Acad. Sci. USA **91:**1406–1410.
2. **Andino, R., G. E. Rieckhof, and D. Baltimore.** 1990. A functional ribonucleoprotein complex forms around the 5′ end of poliovirus RNA. Cell **63:**369–380.
3. **Andino, R., G. E. Rieckhof, P. L. Achacoso, and D. Baltimore.** 1993. Poliovirus RNA synthesis utilizes an RNP complex formed around the 5′-end of viral RNA. EMBO J. **12:**3587–3598.
4. **Barton, D. J., E. P. Black, and J. B. Flanegan.** 1995. Complete replication of poliovirus in vitro: preinitiation RNA replication complexes require soluble cellular factors for the synthesis of VPg-linked RNA. J. Virol. **69:**5516–5527.
5. **Barton, D. J., B. J. Morasco, and J. B. Flanegan.** 1996. Assays for poliovirus polymerase, $3D^{Pol}$, and authentic RNA replication in HeLa S10 extracts. Methods Enzymol. **275:**35–57.
6. **Barton, D. J., B. J. Morasco, and J. B. Flanegan.** 1999. Translating ribosomes inhibit poliovirus negative-strand RNA synthesis. J. Virol. **73:**10104–10112.
7. **Barton, D. J., B. J. O'Donnell, and J. B. Flanegan.** 2001. 5′ cloverleaf in poliovirus RNA is a *cis*-acting replication element required for negative-strand synthesis. EMBO J. **20:**1439–1448.
8. **Birikh, K. R., P. A. Heaton, and F. Eckstein.** 1997. The structure, function and application of the hammerhead ribozyme. Eur. J. Biochem. **245:**1–16.
9. **Brown, D. M., S. E. Kauder, C. T. Cornell, G. M. Jang, V. R. Racaniello, and B. L. Semler.** 2004. Cell-dependent role for the poliovirus 3′ noncoding region in positive-strand RNA synthesis. J. Virol. **78:**1344–1351.
10. **Brown, E., A. J. Zajac, and S. M. Lemon.** 1994. In vitro characterization of an internal ribosomal entry site (IRES) present within the 5′ nontranslated region of hepatitis A virus RNA: comparison with the IRES of encephalomyocarditis virus. J. Virol. **68:**1066–1074.
11. **Brown, E. A., S. P. Day, R. W. Jansen, and S. M. Lemon.** 1991. The 5′ nontranslated region of hepatitis A virus RNA: secondary structure and elements required for translation in vitro. J. Virol. **65:**5828–5838.
12. **Clark, J. M.** 1988. Novel non-templated nucleotide addition reactions catalyzed by procaryotic and eucaryotic DNA polymerases. Nucleic Acids Res. **16:**9677–9686.
13. **Duke, G. M., M. A. Hoffman, and A. C. Palmenberg.** 1992. Sequence and structural elements that contribute to efficient encephalomyocarditis virus RNA translation. J. Virol. **66:**1602–1609.
14. **Friebe, P., V. Lohmann, N. Krieger, and R. Bartenschlager.** 2001. Sequences in the 5′ nontranslated region of hepatitis C virus required for RNA replication. J. Virol. **75:**12047–12057.
15. **Frolov, I., R. Hardy, and C. M. Rice.** 2001. *Cis*-acting RNA elements at the 5′ end of Sindbis virus genome RNA regulate minus- and plus-strand RNA synthesis. RNA **7:**1638–1651.
16. **Gamarnik, A. V., and R. Andino.** 1997. Two functional complexes formed by KH domain containing proteins with the 5′ noncoding region of poliovirus RNA. RNA **3:**882–892.
17. **Ghazi, F., P. J. Hughes, T. Hyypiä, and G. Stanway.** 1998. Molecular analysis of human parechovirus type 2 (formerly echovirus 23). J. Gen. Virol. **79:**2641–2650.
18. **Goodfellow, I. G., C. Polacek, R. Andino, and D. J. Evans.** 2003. The poliovirus 2C *cis*-acting replication element-mediated uridylylation of VPg is not required for synthesis of negative-sense genomes. J. Gen. Virol. **84:**2359–2363.
19. **Herold, J., and R. Andino.** 2000. Poliovirus requires a precise 5′ end for efficient positive-strand RNA synthesis. J. Virol. **74:**6394–6400.
20. **Herold, J., and R. Andino.** 2001. Poliovirus RNA replication requires genome circularization through a protein-protein bridge. Mol. Cell **7:**581–591.
21. **Ishii, T., K. Shiroki, A. Iwai, and A. Nomoto.** 1999. Identification of a new element for RNA replication within the internal ribosome entry site of poliovirus RNA. J. Gen. Virol. **80:**917–920.
22. **Jia, X.-Y., M. Tesar, D. F. Summers, and E. Ehrenfeld.** 1996. Replication of hepatitis A viruses with chimeric 5′ nontranslated regions. J. Virol. **70:**2861–2868.
23. **Koonin, E. V.** 1991. The phylogeny of RNA-dependent RNA polymerases of positive-strand RNA viruses. J. Gen. Virol. **72:**2197–2206.
24. **Le, S.-Y., J.-H. Chen, N. Sonenberg, and J. V. Maizel, Jr.** 1993. Conserved tertiary structural elements in the 5′ nontranslated region of cardiovirus, aphthovirus and hepatitis A virus RNAs. Nucleic Acids Res. **21:**2445–2451.
25. **Lu, H.-H., and E. Wimmer.** 1996. Poliovirus chimeras replicating under the translational control of genetic elements of hepatitis C virus reveal unusual properties of the internal ribosomal entry site of hepatitis C virus. Proc. Natl. Acad. Sci. USA **93:**1412–1417.
26. **Lyons, T., K. E. Murray, A. W. Roberts, and D. J. Barton.** 2001. Poliovirus 5′-terminal cloverleaf RNA is required in *cis* for VPg uridylylation and the initiation of negative-strand RNA synthesis. J. Virol. **75:**10696–10708.
27. **Martin, L. R., and A. C. Palmenberg.** 1996. Tandem mengovirus 5′ pseudoknots are linked to viral RNA synthesis, not poly(C)-mediated virulence. J. Virol. **70:**8182–8186.
28. **Mathews, D. H., J. Sabina, M. Zuker, and D. H. Turner.** 1999. Expanded sequence dependence of thermodynamic parameters improves prediction of RNA secondary structure. J. Mol. Biol. **288:**911–940.
29. **Molla, A., A. V. Paul, and E. Wimmer.** 1991. Cell-free, de novo synthesis of poliovirus. Science **254:**1647–1651.
30. **Morasco, B. J., N. Sharma, J. Parilla, and J. B. Flanegan.** 2003. Poliovirus *cre*(2C)-dependent synthesis of VPgpUpU is required for positive- but not negative-strand RNA synthesis. J. Virol. **77:**5136–5144.
31. **Murray, K. E., and D. J. Barton.** 2003. Poliovirus CRE-dependent VPg uridylylation is required for positive-strand RNA synthesis but not for negative-strand RNA synthesis. J. Virol. **77:**4739–4750.
32. **Murray, K. E., B. P. Steil, A. W. Roberts, and D. J. Barton.** 2004. Replication of poliovirus RNA with complete internal ribosome entry site deletions. J. Virol. **78:**1393–1402.
33. **Nagashima, S., J. Sasaki, and K. Taniguchi.** 2003. Functional analysis of the stem-loop structures at the 5′ end of the Aichi virus genome. Virology **313:**56–65.
34. **Nateri, A. S., P. J. Hughes, and G. Stanway.** 2002. Terminal RNA replication elements in human parechovirus 1. J. Virol. **76:**13116–13122.
35. **Novak, J. E., and K. Kirkegaard.** 1991. Improved method for detecting poliovirus negative strands used to demonstrate specificity of positive-strand encapsidation and the ratio of positive to negative strands in infected cells. J. Virol. **65:**3384–3387.
36. **Parsley, T. B., J. S. Towner, L. B. Blyn, E. Ehrenfeld, and B. L. Semler.** 1997. Poly (rC) binding protein 2 forms a ternary complex with the 5′-terminal sequences of poliovirus RNA and the viral 3CD proteinase. RNA **3:**1124–1134.
37. **Pringle, C. R.** 1999. Virus taxonomy at the XIth International Congress of Virology, Sydney, Australia, 1999. Arch. Virol. **144:**2065–2070.
38. **Racaniello, V. R.** 2001. *Picornaviridae*: the viruses and their replication, p. 685–722. *In* D. M. Knipe, P. M. Howley, D. E. Griffin, R. A. Lamb, M. A. Martin, B. Roizman, and S. E. Straus (ed.), Fields virology, 4th ed. Lippincott-Williams & Wilkins Co., Philadelphia, Pa.
39. **Rivera, V. M., J. D. Welsh, and J. V. Maizel, Jr.** 1988. Comparative sequence analysis of the 5′ noncoding region of the enteroviruses and rhinoviruses. Virology **165:**42–50.
40. **Rohll, J. B., N. Percy, R. Ley, D. J. Evans, J. W. Almond, and W. S. Barclay.** 1994. The 5′-untranslated regions of picornavirus RNAs contain independent functional domains essential for RNA replication and translation. J. Virol. **68:**4384–4391.
41. **Sambrook, J., and D. W. Russell.** 2001. Molecular cloning: a laboratory manual, 3rd ed. Cold Spring Harbor Laboratory Press, Cold Spring Harbor, N.Y.
42. **Sasaki, J., Y. Kusuhara, Y. Maeno, N. Kobayashi, T. Yamashita, K. Sakae, N. Takeda, and K. Taniguchi.** 2001. Construction of an infectious cDNA clone of Aichi virus (a new member of the family *Picornaviridae*) and mutational analysis of a stem-loop structure at the 5′ end of the genome. J. Virol. **75:**8021–8030.
43. **Sasaki, J., and K. Taniguchi.** 2003. The 5′-end sequence of the genome of Aichi virus, a picornavirus, contains an element critical for viral RNA encapsidation. J. Virol. **77:**3542–3548.
44. **Shaffer, D. R., E. A. Brown, and S. M. Lemon.** 1994. Large deletion mutations involving the first pyrimidine-rich tract of the 5′ nontranslated RNA of human hepatitis A virus define two adjacent domains associated with distinct replication phenotypes. J. Virol. **68:**5568–5578.
45. **Shiroki, K., T. Ishii, T. Aoki, M. Kogashi, S. Ohka, and A. Nomoto.** 1995. A new *cis*-acting element for RNA replication within the 5′ noncoding region of poliovirus type 1 RNA. J. Virol. **69:**6825–6832.
46. **Svitkin, Y. V., and N. Sonenberg.** 2003. Cell-free synthesis of encephalomyocarditis virus. J. Virol. **77:**6551–6555.
47. **Yamashita, T., S. Kobayashi, K. Sakae, S. Nakata, S. Chiba, Y. Ishihara, and S. Isomura.** 1991. Isolation of cytopathic small round viruses with BS-C-1 cells from patients with gastroenteritis. J. Infect. Dis. **164:**954–957.
48. **Yamashita, T., K. Sakae, H. Tsuzuki, Y. Suzuki, N. Ishikawa, N. Takeda, T. Miyamura, and S. Yamazaki.** 1998. Complete nucleotide sequence and genetic organization of Aichi virus, a distinct member of the *Picornaviridae* associated with acute gastroenteritis in humans. J. Virol. **72:**8408–8412.
49. **Yamashita, T., M. Ito, Y. Kabashima, H. Tsuzuki, A. Fujiura, and K. Sakae.** 2003. Isolation and characterization of a new species of kobuvirus associated with cattle. J. Gen. Virol. **84:**3069–3077.
50. **Zell, R., K. Sidigi, A. Henke, J. Schmidt-Brauns, E. Hoey, S. Martin, and A. Stelzner.** 1999. Functional features of the bovine enterovirus 5′-non-translated region. J. Gen. Virol. **80:**2299–2309.

Available online at www.sciencedirect.com
SCIENCE DIRECT®
Journal of Virological Methods 126 (2005) 165–169
Journal of Virological Methods
www.elsevier.com/locate/jviromet

Complete nucleotide sequences of two RNA segments of human picobirnavirus

Mitsutaka Wakuda [a], Yaowapa Pongsuwanna [b], Koki Taniguchi [a,*]

[a] *Department of Virology and Parasitology, Fujita Health University, School of Medicine, Toyoake, Aichi 470-1192, Japan*
[b] *Enteric and Respiratory Viruses Laboratory, National Institute of Health, Department of Medical Sciences, Nonthaburi 11000, Thailand*

Received 27 September 2004; received in revised form 7 February 2005; accepted 9 February 2005
Available online 25 March 2005

Abstract

Picobirnaviruses are unclassified, non-enveloped, spherical, small viruses with a genome comprising two double-stranded RNA segments. Only incomplete sequence data on picobirnaviruses are available so far. By cloning involving single primer amplification, full-length cDNAs were prepared corresponding to RNA segments 1 and 2 of a picobirnavirus (strain Hy005102) isolated from a stool specimen from an infant with acute non-bacterial gastroenteritis in Thailand, and the complete nucleotide sequences were determined. RNA segments 1 and 2 are 2,525 and 1,745 base pairs in length, respectively. RNA segment 1 encodes two open reading frames (ORFs) of 224 and 552 amino acids, and RNA segment 2 codes for a single ORF of 534 amino acids. On comparison with a part of the nucleotide sequences of the RNA segment, 2 of the other published picobirnavirus strains, the Thai strain was found to be related most closely to one of the US strains.

Keywords: Picobirnavirus; Gastroenteritis; Nucleotide sequence; Double-stranded RNA

Picobirnaviruses were first detected in fecal specimens from humans and rats in 1988 (Pereira et al., 1988a,b). The virus particles are 35–41 nm in diameter and non-enveloped, with a buoyant density of 1.38–1.40 g/ml in cesium chloride. The genome consists of two double-stranded (ds) RNA segments of 2.3–2.6 and 1.5–1.9 kilobase pairs (kbp), respectively. Segment 2 encodes RNA-dependent RNA polymerase, and segment 1 appears to code for capsid protein. The RNA electropherotypes on polyacrylamide gel electrophoresis (PAGE) of human picobirnaviruses are variable, suggesting RNA heterogeneity among strains. Picobirnaviruses have been detected in feces from pigs (Gatti et al., 1989; Ludert et al., 1991; Pongsuwanna et al., 1996), guinea pigs (Pereira et al., 1989), rabbits (Gallimore et al., 1993; Ludert et al., 1995), hamsters, rats, giant anteaters (Haga et al., 1999), foals, calves, and chickens (Alfieri et al., 1988; Leite et al., 1990), as well as humans (Banyai et al., 2003; Cascio et al., 1996; Chandra, 1997; Gallimore et al., 1995a; Grohmann et al., 1993; Liste et al., 2000; Ludert and Liprandi, 1993; Martinez et al., 2003; Pereira et al., 1988a). Most picobirnaviruses, particularly those of human origin, have been detected in stools from gastroenteritis patients in the process of PAGE of virus RNA for the detection of rotaviruses, major agents causing non-bacterial gastroenteritis. However, the frequency of detection of picobirnaviruses varies in various investigations, and the role of the viruses as a cause of gastroenteritis has not yet been established. In one study (Cascio et al., 1996), picobirnaviruses were identified in 0.4% (3/690) and 0% (0/92) of stool specimens from humans with and without gastroenteritis, respectively, while in another study (Gallimore et al., 1995b), picobirnaviruses were detected at almost equal frequencies (13% and 12%) in humans with and without gastroenteritis, respectively. In HIV-positive patients, the association of picobirnaviruses with gastroenteritis has been implicated (Grohmann et al., 1993; Liste et al., 2000). In some studies (Banyai et al., 2003; Rosen et al., 2000), stool samples positive for picobirnaviruses were also positive for

* Corresponding author. Tel.: +81 562 93 2467; fax: +81 562 93 4008.
E-mail address: kokitani@fujita-hu.ac.jp (K. Taniguchi).

0166-0934/$ – see front matter © 2005 Elsevier B.V. All rights reserved.
doi:10.1016/j.jviromet.2005.02.010

norovirus. Thus, the possibility cannot be excluded that picobirnaviruses might be secondary opportunistic pathogens or innocuous viruses in the intestine. More information is required on picobirnaviruses including sequence data to determine whether or not picobirnaviruses play a significant role in gastroenteritis.

Picobirnaviruses have also been detected in the oocysts of *Cryptosporidium parvum* and in human stools containing *Cryptosporidium parvum* (Gallimore et al., 1995a; Green et al., 1999; Khramtrov et al., 1997). The picobirnaviruses are named atypical picobirnaviruses, and have properties similar to those of the so-called typical picobirnaviruses mentioned above. However, an atypical picobirnavirus has a smaller genome, and the RNA electropherotypes among the isolates from stools are highly consistent (Khramtrov et al., 2000). The sequences of two dsRNA segments from the cytoplasm of *Cryptosporidium parvum* sporozoites have been reported. The two RNA segments are of 1786 bp and 1374 bp, and each has one large ORF comprising 1704 and 963 nucleotides, respectively (Khramtrov et al., 1997). In contrast to those of typical picobirnaviruses, segment 1 has an ORF for viral RNA polymerase, and segment 2 may encode a capsid protein. Thus, there is a marked difference in the nucleotide sequences between typical and atypical picobirnaviruses.

Although several reports on the nucleotide sequences of typical human picobirnaviruses have appeared (Banyai et al., 2003; Martinez et al., 2003; Rosen et al., 2000), most studies revealed only parts of the nucleotide sequences; except that Rosen et al. (2000) reported the nucleotide sequences of a part of RNA segment 1 and the nearly full-length of RNA segment 2 of a human picobirnavirus. In this study, the complete nucleotide sequences of segments 1 and 2 of a human picobirnavirus was determined by obtaining the full-length cDNAs by means of the single primer cloning method developed by Lambden et al. (1992).

1. Materials and methods

1.1. Viruses

A stool specimen containing picobirnavirus was obtained from an infant with acute non-bacterial gastroenteritis in Thailand. A 20% (w/v) of stool suspension was prepared in phosphate-buffered saline (PBS). A simian rotavirus SA11 was employed as a reference segmented dsRNA virus for confirming the validity of the methodology of single primer amplification and the subsequent cloning.

1.2. cDNA cloning

RNA was extracted from 20% stool suspension in PBS using ISOGEN-LS (Nippon Gene Ltd.). Cloning was performed based on the method described by Lambden et al. (1992) with some modifications. Primer A (5′ CCC TCG AGT ACT AAC TAG TTA ACT GAT CAC CTC TAG ACC TTT 3′), whose 5′ end was phosphorylated and whose 3′ end incorporated an NH_2 blocking group, was ligated to the 3′ end of the viral RNA. Ligation was carried out for 16 h at 8 °C in 50 μl reaction mixture using a TaKaRa ligation kit. The mixture was purified with microcon-100 (Amicon). The RNA was suspended in a 25 μl solution containing 40 pmol of primer B (5′ AAA GGT CTA GAG GTG ATC AGT TAA CTA GTT AGT ACT CGA GGG 3′), 8% dimethyl sulfoxide, and 1.6 mM dNTP. The RNA was denatured at 97 °C for 3 min, at 70 °C for 10 min, and at 60 °C for 5 min. Reverse transcription was performed at 60 °C for 1 h in cDNA synthesis buffer containing 5 mM dithiothreitol, 22.5 U of THERMO SCRIPT reverse transcriptase (Invitrogen), and 80 U of RNase inhibitor. Two-step PCR (first and second PCR) was carried out using Ex Taq polymerase (TaKaRa), as follows. First PCR with primer C (5′ GGT CTA GAG GTG ATC AGT TAA CTA GTT AGT ACT C 3′) was carried out with initial denaturation at 95 °C for 2 min, 10 PCR cycles (95 °C for 1 min, 60 °C for 45 s, and 72 °C for 2 min 30 s), and then further 20 PCR cycles with 10 s cycle extension during each elongation step. Second PCR with primer D (5′ TCA GTT AAC TAG TTA GTA CTC GAG GG 3′) involved 10 PCR cycles (95 °C for 1 min, 60 °C for 45 s, and 72 °C for 2 min 30 s), and then further 15 PCR cycles with 10 s cycle extension during each elongation step. The final PCR product was subjected to 1% agarose gel electrophoresis, and the DNA band corresponding to each of segments 1 and 2 was excised. The DNA was purified with Wizard SV gel and a PCR Clean-Up system (Promega), and then cloned into the PCR-TOPO vector in a TOPO TA Cloning kit (Invitrogen). Six clones for each of segments 1 and 2 were selected and used for sequencing.

1.3. Nucleotide sequence determination

The nucleotide sequences of both strands of the cloned picobirnavirus gene segments (six clones for each of segments 1 and 2) were determined using an ABI Prism BigDye Terminator Cycle Sequencing Ready Reaction Kit (Perkin–Elmer Corp.) and an automated sequencer (Applied Biosystems Model 310; Applied Biosystems, Foster City, CA). Primers complementary to the T7 and SP6 promoters of the PCR-TOPO vector were used to obtain initial sequence data, and primers in subsequent sequence reactions were prepared based on sequence data obtained by the preceding analysis. Sequence analysis and comparisons were performed using GENETYX-MAC (Ver.10).

1.4. Nucleotide sequence accession numbers

The nucleotide sequence data reported in this paper appear in the DDBJ, EMBL and GeneBank nucleotide sequence database under the accession numbers AB186897 (segment 1) and AB186898 (segment 2).

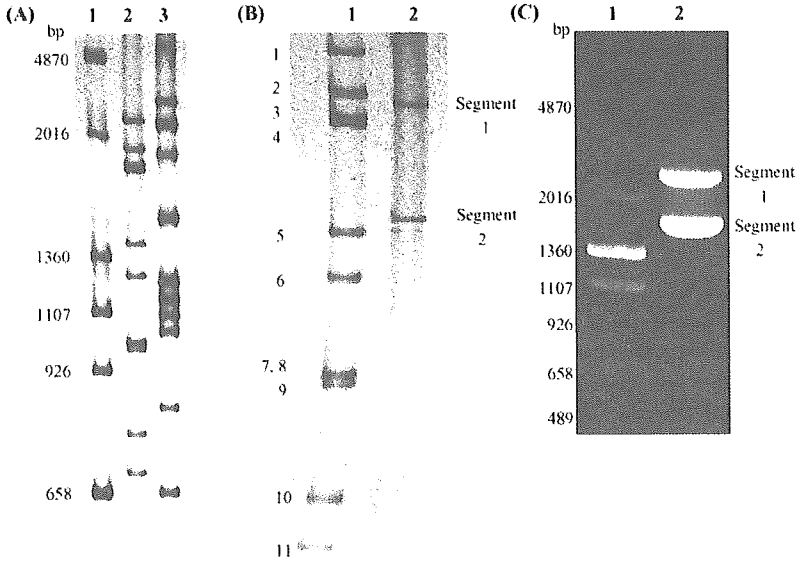

Fig. 1. (A) Profile of cDNA products amplified from SA11 rotavirus dsRNA on PAGE. Lane 1, DNA size markers (pHY marker; TaKaRa); lane 2, SA11 dsRNA; lane 3, amplified SA11 cDNA products. (B) RNA profile of human picobirnavirus (strain Hy005102) from a stool specimen on PAGE. Lane 1, SA11; lane 2, Hy005102. (C) Profile of cDNA products amplified from human picobirnavirus dsRNA in agarose gel. Lane 1, DNA size markers (pHY marker; TaKaRa); lane 2, amplified picobirnavirus cDNA products.

2. Results and discussion

Using a simian rotavirus strain SA11, the validity of the method for amplifying dsRNA segments described originally by Lambden et al. (1992) was examined. As shown in Fig. 1A, all the 11 RNA segments were consistently amplified. It was noted that the electrophoretic pattern of the 11 cDNA segments on PAGE was distinct from that of the original 11 dsRNA segments. This method was applied to the cloning of two RNA segments from a picobirnavirus. Fig. 1B shows the RNA electrophoretic profile on PAGE of the RNA segments of a Thai picobirnavirus strain, Hy005102, obtained from a stool specimen. On single primer amplification, it was suggested that full-length DNAs corresponding to the two segments of the picobirnavirus were clearly amplified based on the electrophoretic mobility of DNA bands (Fig. 1C). Using the DNA purified from the agarose gel, six clones of each of segments 1 and 2 were selected after TA cloning, and then subjected to nucleotide sequence determination.

RNA segment 1 is 2525 nt in length. The GC content is 45.8%, although the 5′ non-coding region is AU-rich (GC content: 36.5%). A polyadenylation signal AAUAAA was not found. We confirmed the nucleotide sequence of the segment 1 obtained from the cDNA prepared by the cloning using single-primer amplification method by sequencing the DNA products obtained by a standard RT-PCR with 5′ and 3′ terminal primers prepared based on the sequences found in this study. As shown in Fig. 2, the sequence has two long open-reading frames (ORF1 and ORF2). ORF1 begins with AUG at positions 157–159 and terminates at positions 829–831, and ORF2 begins with AUG at positions 828–830 and terminates at positions 2484–2486. Two nucleotides, UG at positions 829 and 830 overlap as part of a termination codon for ORF1 and part of an initiation codon for ORF2, although the pos-

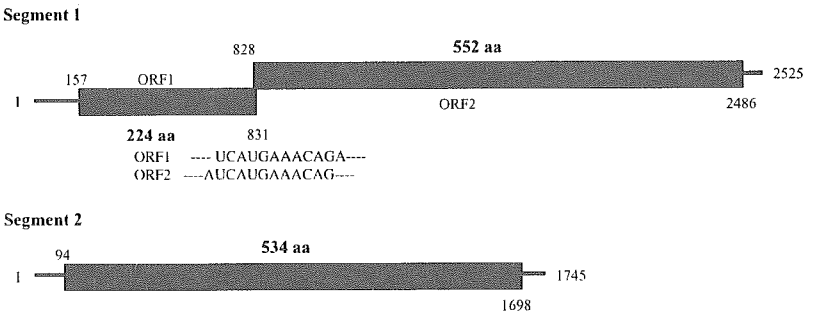

Fig. 2. Genome organization of segments 1 and 2 of human picobirnavirus. The termination codon (UGA) for ORF1 and the initiation codon (AUG) for ORF2 in segment 1 are overlapped.

sibility of the occurrence of −1 frameshifting at this site can not be excluded. ORF1 codes for a hydrophilic 224-amino acid protein with an estimated molecular weight of 24.9 kDa, and ORF2 encodes a 552-amino acid protein of 62 kDa. The p*I* values of the 24.9 kDa and 62 kDa proteins are 9.03 and 5.74, respectively. The 62 kDa protein was found to have a highly hydrophilic N-terminus domain comprising about 50 amino acids rich in arginine and lysine; the remaining part being hydrophobic. There has been no report on the protein profile of picobirnavirus. Any amino acid motifs suggesting protein function could not be detected in ORF1 and ORF2. By preliminary in vitro transcription/translation experiments (TNT reticulocyte lysate system; Promega, Madison, Wis.), a 25 kDa protein corresponding to the ORF1 of the segment 1 was detected, while a 62 kDa protein band, which is expected to be synthesized from the ORF2 of the segment 1 could not be detected (Wakuda and Taniguchi, unpublished data). The initiation codon of the ORF2 might be weak in the system employed in this study. Further studies including the preparation of virus-like particles by baculovirus expression system are required to determine whether or not the predicted ORFs are authentic and whether or not the ORFs encodes a polyprotein.

Rosen et al. (2000) reported that although the estimated full-length RNA segment 1 of a human strain 3-GA-91 was approximately 2300 bp, on the basis of its electrophoretic mobility on PAGE, the clone obtained was only 1572 bp in length. On comparison of the nucleotide sequences between strain Hy005102 and strain 3-GA-91, the identity was found to be 49.7%. The RNA segment 1 of a rabbit picobirnavirus (strain 35227/89) was found to be 2362 bp in length (Green et al., 1999). The gene encodes a major open reading frame (ORF1) of 591 amino acids and two smaller ORFs (ORF2: 212–532 and ORF3: 51–215) amino acids. The nucleotide identity between strains Hy005102 and 35227/89 is 46.2%. The RNA segments of *Cryptosporidium parvum* are 1786 bp (ORF: 1704 bp) and 1374 bp (ORF: 963 bp) in length (Khramtrov et al., 1997). RNA segments 1 and 2 of *Cryptosporidium parvum* code for RNA–RNA polymerase and capsid protein, respectively. No significant identity was found between typical and atypical picobirnaviruses as reported previously.

The complete nucleotide sequence of segment 2 was also determined (Fig. 2). The segment 2 nucleotide sequence of the strain Hy005102 is 1,745 bases long, and contains a single long ORF beginning with AUG at positions 94–96 and terminating with UGA at positions 1,696–1,698. The GC content is 46.4%, the 5′ non-coding region is AU-rich (GC content: 22.6%), as found for segment 1, and the 5′ end five nucleotides, GUAAA, are conserved in segments 1 and 2. The sequence was confirmed by sequencing the cDNA product prepared by the standard RT-PCR with picornavirus RNA as a template and 5′ and 3′ terminal primers prepared based on the sequences found in this study. The ORF encodes 534 amino acids with a molecular weight of 60 kDa, and the p*I* value is 8.13. In a previous study (Rosen et al., 2000), segment 2 was suggested to encode RNA–RNA polymerase. Segment 2 of strain Hy005102 retains the three motifs identified in RNA-dependent RNA polymerases of dsRNA and some single-stranded RNA viruses. By in vitro transcription/translation experiments (TNT reticulocyte lysate system; Promega, Madison, Wis.) using the plasmid containing segment 2 cDNA, a 60 kDa protein corresponding to the ORF product of segment 2 was detected (Wakuda and Taniguchi, unpublished data).

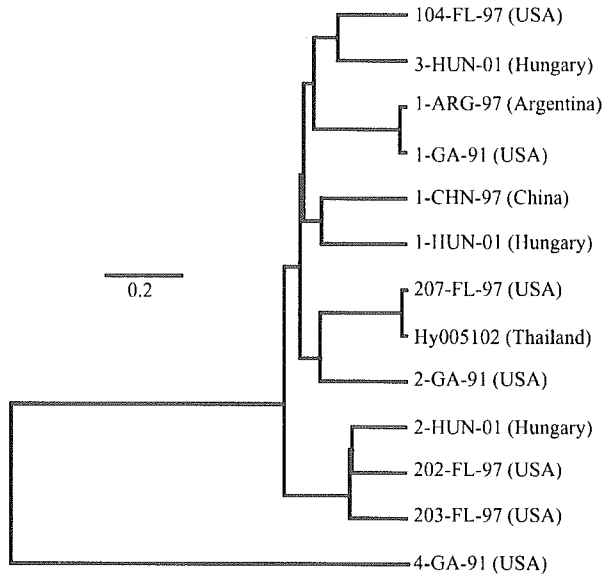

Fig. 3. Phylogenetic tree for a part of the nucleotide sequences (168 bp; positions 714–881) of RNA segment 2 of human picobirnaviruses. The tree was constructed using the unweighted pair group method with arithmetic means. The bar indicates the variation scale.

The published sequences of segment 2 for strains 4-GA-91 (genogroup II) and 1-CHN-97 (genogroup I) are 1,674 bp and 1,696 bp in length (Rosen et al., 2000). RNA segment 2 of a rabbit picobirnavirus is 1.85 kbp in length (Green et al., 1999). On comparative analysis of the segment 2 nucleotides, strain Hy005102 exhibited 61.4% and 44.5% identity with strains 1-CHN-97 and 4-GA-91, respectively. The deduced amino acid sequence identities of strain Hy005102 were 61.6% and 21.5% with strains 1-CHN-97 and 4-GA-91, respectively. However, no significant identity was found in the segment 2 sequence between strain Hy005102 and rabbit picobirnavirus strains 35227/89.

Sequence information on picobirnaviruses is limited. Using only a small part (168 nucleotides; positions from 714–881) of segment 2 sequences, a phylogenetic tree was constructed. As shown in Fig. 3, the Thai strain, Hy005102, was most closely related to a US strain, 207-FL-97 (identity: 97.6%), in comparison with other picobirnaviruses (identities: 48.9%–71.0%).

The quantity of picobirnavirus particles in stools is very small and there are no systems for cultivation of the viruses in experimental animals or cell cultures yet. In order to determine the etiological role of human picobirnaviruses, epi-

demiological surveys including prevalence of the viruses and antibodies are required. Information on the complete nucleotide sequence of the genome of the picobirnavirus will be helpful for preparing self-assembled virus-like particles and their hyper-immune serum for surveys on the prevalences of picobirnavirus and its antibody and for undertaking RT-PCR surveys of picobirnavirus prevalence more efficiently.

Acknowledgment

This work was partially supported by a Grant-in-Aid for Scientific Research and for the Open Research Center Program from the Ministry of Education, Culture, Sports, Science and Technology of Japan.

References

Alfieri, A.F., Alfieri, A., Resende, J.S., Resende, M., 1988. A new bisegmented double-stranded RNA virus in avian feces. Arq. Bras. Med. Vet. Zootec. 40, 437–440.

Banyai, K., Jakab, F., Reuter, G., Bene, J., Uj, M., Melegh, B., Szucs, G., 2003. Sequence heterogeneity among human picobirnaviruses detected in a gastroenteritis outbreak. Arch. Virol. 148, 2281–2291.

Cascio, A., Bosco, M., Vizzi, E., Giamanco, A., Ferraro, D., Arista, S., 1996. Identification of picobirnavirus from faeces of Italian children suffering from acute diarrhea. Eur. J. Epidemiol. 12, 545–547.

Chandra, R., 1997. Picornavirus, a novel group of undescribed viruses of mammals and birds: a minireview. Acta Virol. 41, 59–62.

Gallimore, C.I., Appleton, H., Lewis, D., Green, J., Brown, D.W.G., 1995a. Detection and characterization of bisegmented double-stranded RNA viruses (picornaviruses) in human faecal specimens. J. Med. Virol. 45, 135–140.

Gallimore, C.I., Green, J., Casemore, D.P., Brown, D.W., 1995b. Detection of a picornavirus associated with *Cryptosporidium* positive stools from humans. Arch. Virol. 140, 1275–1278.

Gallimore, C., Lewis, D., Brown, D., 1993. Detection and characterization of a novel bisegmented double-stranded RNA virus (picobirnavirus) from rabbit faeces. Arch. Virol. 133, 63–73.

Gatti, M.S.V., De Castro, A.F.P., Ferraz, M.M.G., 1989. Viruses with bisegmented double-stranded RNA in pig faeces. Res. Vet. Sci. 47, 397–398.

Green, J., Gallimore, C.I., Clewley, J.P., Brown, D.W.G., 1999. Genomic characterization of the large segment of a rabbit picobirnavirus and comparison with the atypical picornavirus of *Cryptosporidium parvum*. Arch. Virol. 144, 2457–2465.

Grohmann, G.S., Glass, R.I., Pereira, H.G., Monroe, S.S., Hightower, A.W., Weber, R., Brvan, R.T., 1993. Enteric viruses and diarrhea in HIV-infected patients enteric opportunistic infections working group. N. Engl. J. Med. 329, 14–20.

Haga, I.R., Martins, S.S., Hosomi, S.T., Vicentini, F., Tanaka, H., Gatti, M.S., 1999. Identification of a bisegmented double-stranded RNA virus (picobirnavirus) in faeces of giant anteaters. Vet. J. 158, 234–236.

Khramtrov, N.V., Woods, K.M., Nesterenko, M.V., Dykstra, C.C., Upton, S.J., 1997. Virus-like, double-stranded RNAs in the parasitic protozoan *Cryptosporidium parvum*. Mol. Microbiol. 36, 289–300.

Khramtrov, N.V., Chung, P.A., Dykstra, C.C., Griffiths, J.K., Morgan, U.M., Arrowood, M.J., Upton, S.J., 2000. Presence of double-stranded RNAs in human and calf isolates of *Cryptosporidium parvum*. J. Parasitol. 86, 275–282.

Lambden, P.R., Cooke, S.J., Caul, E.O., Clarke, I.N., 1992. Cloning of non-cultivatable human rotavirus by single-primer amplification. J. Virol. 66, 1817–1822.

Leite, J.P.G., Monteiro, S.P., Fialho, A.M., Pereira, H.G., 1990. A novel avian virus with trisegmented double-stranded RNA and further observations on previously described similar viruses with bisegmented genome. Virus Res. 16, 119–126.

Liste, M.B., Natera, I., Suarez, J.A., Pujol, F.H., Liprandi, F., Ludert, J.E., 2000. Enteric virus infections and diarrhea in healthy and human immunodeficiency virus-infected children. J. Clin. Microbiol. 38, 2873–2877.

Ludert, J.E., Abdul-Latiff, L., Liprandi, A., Liprandi, F., 1995. Identification of picobirnavirus, viruses with bisegmented double-stranded RNA in rabbit faeces. Res. Vet. Sci. 59, 222–225.

Ludert, J.E., Hidalgo, M., Gil, F., Liprandi, F., 1991. Identification in porcine faeces of a novel virus with a bisegmented double-stranded RNA genome. Arch. Virol. 117, 97–107.

Ludert, J.E., Liprandi, F., 1993. Identification of viruses with bi- and trisegmented double-stranded RNA genome in faeces of children with gastroenteritis. Res. Virol. 144, 219–224.

Martinez, L.C., Giordano, M.O., Isa, M.B., Alvarado, L.F., Pavan, J.V., Rinaldi, D., Nates, S.V., 2003. Molecular diversity of partial-length genomic segment 2 of human picornavirus. Intervirology 46, 207–213.

Pereira, H.G., De Araujo, H.P., Fialho, A.M., De Castro, L., Monteiro, S.P., 1989. A virus with bisegmented double-stranded RNA genome in guinea pig intestines. Mem. Inst. Oswaldo Cruz. 84, 137–140.

Pereira, H.G., Fialho, A.M., Flewett, T.H., Teixeira, J.M.S., Andrade, Z.P., 1988a. Novel viruses in human faeces. Lancet 2, 103–104.

Pereira, H.G., Flewett, T.H., Candeias, J.A., Barth, O.M., 1988b. A virus with a bisegmented double-stranded RNA genome in rat (*Oryzomys nigripes*) intestines. J. Gen. Virol. 69, 49–54.

Pongsuwanna, Y., Taniguchi, K., Chiwakul, M., Urasawa, T., Wakasugi, F., Javayasu, C., Urasawa, S., 2000. Serological and genomic characterization of porcine rotaviruses in Thailand: detection of G10 porcine rotavirus. J. Clin. Microbiol. 34, 1050–1057.

Rosen, B.I., Fang, Z-Y., Glass, R.I., Monroe, S.S., 2000. Cloning of human picobirnavirus genomic segments and development of an RT-PCR detection assay 277, 316–329.

Journal of Medical Virology 76:129–136 (2005)

Expression and Antigenicity of Virus-Like Particles of Norovirus and Their Application for Detection of Noroviruses in Stool Samples

Kunio Kamata,[1,2] Kuniko Shinozaki,[3] Mineyuki Okada,[3] Yoshiyuki Seto,[4] Shinichi Kobayashi,[5] Kenji Sakae,[5] Mitsuaki Oseto,[6] Katsuro Natori,[7] Haruko Shirato-Horikoshi,[8] Kazuhiko Katayama,[7] Tomoyuki Tanaka,[8] Naokazu Takeda,[7] and Koki Taniguchi[2]*

[1]*Technical Marketing Department, Denka-Seiken Co., Ltd., Gosen, Niigata, Japan*
[2]*Department of Virology and Parasitology, Fujita Health University School of Medicine, Toyoake, Aichi, Japan*
[3]*Laboratory of Virology, Public Health Laboratory of Chiba Prefecture, Chuoh-ku, Chiba, Japan*
[4]*Department of Virology, Osaka City University Medical School, Abeno-ku, Osaka, Japan*
[5]*Aichi Prefectural Institute of Public Health, Tujimachi, Kita-ku, Nagoya, Japan*
[6]*Ehime Prefectural Institute of Public Health and Environment Science 8-234,Sanbancho, Matsuyama, Ehime, Japan*
[7]*Department of Virology II, National Institute of Infectious Diseases, Musashi-Murayama, Tokyo, Japan*
[8]*Sakai City Institute of Public Health, Sakai, Osaka, Japan*

Human noroviruses (NoVs), members of the genus *Norovirus* in the family *Caliciviridae*, are the leading agents of nonbacterial acute gastroenteritis worldwide. Human NoVs are currently divided into at least two genogroups, genogroup I (GI) and genogroup II (GII), each of which contains at least 14 and 17 genotypes. To explore the genetic and antigenic relationship among NoVs, we expressed the capsid protein of four genetically distinct NoVs, the GI/3 Kashiwa645 virus, the GII/3 Sanbu809 virus, the GII/5 Ichikawa754 virus, and the GII/7 Osaka10-25 virus in baculovirus expression system. An antigen enzyme-linked immunosorbent assay (ELISA) with hyperimmune serum against the four recombinant capsid proteins and characterized previously three capsid proteins derived from GI/1, GI/4, and GII/12 was developed to detect the NoVs antigen in stools. The antigen ELISA was highly specific to the homotypic strains, allowing assignment of a strain to a Norovirus genetic cluster within a genogroup. ***J. Med. Virol. 76:129–136, 2005.*** © 2005 Wiley-Liss, Inc.

KEY WORDS: norovirus; ELISA; gastroenteritis; virus-like particle; calicivirus

INTRODUCTION

Norovirus (NoV), a member of one of four genera in the family *Caliciviridae* [Atmar and Estes, 2001; Green et al., 2001a], is a major cause of water and food-borne acute nonbacterial gastroenteritis, and is composed of many genetically distinct viruses. [Kapikian, 1994; Kapikian et al., 1996; Estes et al., 1997]. The detection and molecular characterization of NoV have been hampered due to the lack of cell culture and small animal models [Duizer et al., 2004]. However, recent progress in molecular cloning and the sequence determination of RNA-dependent RNA polymerase and capsid protein genes of the NoVs has enabled us to classify NoVs into at least two genogroups: genogroup I (GI) and genogroup II (GII) [Green et al., 2001b]. In a previous study, a scheme for genotyping based on the N-terminal capsid protein was demonstrated [Katayama et al., 2002], and a recent report proposed that GI and GII contain at least 14 and 17 genotypes, respectively [Kageyama et al., 2004].

The NoV contains a single-stranded positive-sense RNA genome of 7.6 kb excluding the poly-A tail that encodes three open reading frames (ORFs) [Jiang et al., 1993; Lambden et al., 1993]. ORF1 encodes a nonstructural polyprotein, which is cleaved into functional proteins by a virus-encoded 3C-like protease, and ORF2 and ORF3 encode the major capsid protein VP1 and minor capsid protein VP2, respectively [Jiang et al., 1992; Glass et al., 2000]. When the ORF2 gene alone or the 3′ end of 2.3 kb, including ORF2, ORF3, and the 3′ noncoding region is expressed by a recombinant

Grant sponsor: Ministry of Health, Labor, and Welfare of Japan.

*Correspondence to: Koki Taniguchi, Department of Virology and Parasitology, Fujita Health University School of Medicine, Toyoake, Aichi 470-1192, Japan. E-mail: kokitani@fujita-hu.ac.jp

Accepted 10 January 2005

DOI 10.1002/jmv.20334

Published online in Wiley InterScience (www.interscience.wiley.com)

baculovirus, the recombinant protein spontaneously self-assembles into virus-like particles (VLPs) which are antigenically and morphologically similar to the native virion [Jiang et al., 1992, 2002; Lew et al., 1994a,b; Dingle et al., 1995; Hale et al., 1999; Kobayashi et al., 2000a,b,c; Belliot et al., 2001]. The VLPs have been used successfully for in structural studies [Prasad et al., 1994, 1999], as well as the development of enzyme-linked immunosorbent assay (ELISA) for serological diagnosis of NoV infection [Gray et al., 1993; Green et al., 1993; Parker et al., 1993, 1994, 1995]. Though antigen ELISA using hyperimmune antisera raised against the VLPs has been developed to detect NoV in stools [Graham et al., 1994; Jiang et al., 1995a,b,c; Hale et al., 1999], the sensitivity is low due to the ability of the ELISA to detect only strains closely related to one used to produce the hyperimmune serum [Numata et al., 1994; Jiang et al., 1995a,b,c]. The expression of antigenically distinct more VLPs and the preparation of antisera to them are needed to clarify the antigenic relationship among NoVs.

The expression of four capsid proteins from the GI/3, GII/3, GII/5 and GII/7 NoVs and the preparation of the VLPs are described and the antigenic relationship among seven VLPs, including three NoV VPLs from GI/1, G1/4, and GII/12 prepared previously [Kobayashi et al., 2000a,b,c], and the detection of NoVs in fecal specimens by using an ELISA are described.

MATERIALS AND METHODS

Viruses, RT-PCR, and molecular cloning. Hu/NV/GI/Kashiwa645/1999/JP (Kashiwa645, sequence accession number BD011871), Hu/NV/GII/Sanbu809/1998/JP (Sanbu809, BD011876), and Hu/NV/GII/Ichikawa745/1998/JP (Ichikawa745, BD011877) were associated with outbreaks of acute gastroenteritis as reported by the Kashiwa, Sanbu, and Ichikawa Health Centers in Chiba prefecture, Japan in 1989–1999. Hu/NV/GII/Osaka10-25/1999/JP (Osaka10-25, BD011881) was associated with an outbreak of acute gastroenteritis in Osaka Prefecture, Japan, in 1999. Stool samples containing these viruses were homogenized in phosphate buffered saline (PBS), and a 10% suspension was prepared. After centrifugation at 3,000*g* for 10min, the supernatant was used for RNA extraction with Trizol™ (Gibco BRL, Gaithersburg, MD) [Kobayashi et al., 2000a]. The cDNA synthesis was performed with an oligo-dT15 (Promega Co., Madison, WI) and reverse transcriptase from the Molony murine leukemia virus (Gibco BRL) as described by Green et al. [1997]. An approximately 1.6 kb fragment that encodes the entire VP1 of Kashiwa645, Sanbu809 and Ichikawa745, and a 2.3 kb fragment that encodes the VP1, VP2, 3′ noncoding region, and poly-A of Osaka10-25 were amplified with the primers shown in Table I. The PCR was performed in 100 μl of the reaction mixture containing 2.5 U of Takara Ex Taq (TaKaRa Shuzo Co., Ltd., Kyoto), 10 μl of 10 × PCR buffer, 8 μl of 25 mM dNTPs, 1 μl of 50 μM of each primer, and 5 μl of cDNA. After an initial denaturation at 94°C for 5 min, 35 cycles of amplification were performed using the GeneAmp PCR System 9600 (PE Biosystems, Foster City, CA). Each cycle consisted of denaturation at 94°C for 1 min, primer annealing at 55°C for 1 min, and extension reaction at 72°C for 2 min followed by final extension at 72°C for 7 min. The amplified fragments were cloned into a pCR2.1 plasmid (Invitrogen, San Diego, CA). The nucleotide sequences were determined with an ABI PRISM 310 Genetic Analyzer (Applied Biosystems, Foster City, CA) and phylogenetically analyzed as described previously [Katayama et al., 2002; Kageyama et al., 2004].

Recombinant VLPs

The amplified fragment was isolated from the vector by digestion with the appropriate restriction endonucleases, and inserted into a baculovirus transfer vector pVL1392 (Pharmingen, San Diego, CA), which was used to cotransfect the Sf9 cells (Riken Cell Bank, Tsukuba) with linearized wild-type *Autographa californica* nuclear polyhedrosis virus DNA (Pharmingen) by the lipofectin-mediated method, as described by the manufacturer (Invitrogen). Recombinant baculoviruses thus obtained were selected by two rounds of plaque purification and used to prepare the seed viruses. Tn5 cells (Invitrogen) were infected with the seed virus at a multiplicity of infection (m.o.i.) of 10, incubated at 26.5°C, and the culture medium was harvested at 5–6 days post infection (p.i.). Leupeptin 10 μM (Sigma Chemicals, St. Louis, MO) and 2 μM pepstatin A (Sigma Chemicals) were added to the medium at 3 days p.i. The expression of the recombinant protein in the medium was monitored by sodium dodecyl sulfate-10% polyacrylamide gel electrophoresis (SDS–PAGE) followed by staining with Coomassie brilliant blue. The culture medium was clarified by centrifugation at 10,000*g* for 30 min, and then the VLPs in the supernatant were concentrated by centrifugation at 100,000*g* for 4 hr in a Beckman SW27 rotor. The pellet was resuspended in Grace's medium (DIFCO, Franklin Lakes, New Jersey) and examined by electron microscopy (EM). The VLPs were further purified by $CsCl_2$ equilibrium gradient density gradient centrifugation at 100,000*g* for 24 hr at

TABLE I. Primer Sequences

NoV	Forward primer	Reverse primer
Kashiwa 645	G1/F2 (5′-AATGATGATGGCGTCTAAAGGA-3′)	707R1 (5′-TGAGCCATTATGATCTTCTGATGC-3′)
Sanbu 809	G2/F3 (5′-TTGTGAATGAAGATGGCGTCGA-3′)	MVR1 (5′-AATTATTGAATCCTTCTACGCCCG-3′)
Ichikawa 754	G2/F3 (5′-TTGTGAATGAAGATGGCGTCGA-3′)	SMVR1 (5′-AATTACTGAACCCTTCTACGCCCATTTC-3′)
Osaka 10–25	G2FCR7 (5′-ATGAAGATGGCGTCGAATGACG-3′)	Oligo-dT(33)

16°C. The purified VLPs were used to immunize the animals.

Hyperimmune Sera

Hyperimmune sera to recombinant Kashiwa645 VLPs (r645), Sanbu809 VLPs (r809), Ichikawa754 VLPs (r754), and Osaka10-25 VLPs (r10-25) were prepared in rabbits. The first subcutaneous injection was performed with the purified 500 μg VLPs in Freund's complete adjuvant. After 3 weeks, the animals received two or three booster injections of 250 μg of the VLPs in Freund's incomplete adjuvant at intervals of 1 week. The animals were bled 1 week after the last booster injection. The antibody titers of rabbit hyperimmune sera to VLPs were tested in parallel by an indirect ELISA, as described previously for rSeto 124 VLPs [Kobayashi et al., 2000b] except that a VLP concentration of 0.5 μg/ml was used to coat the ELISA plate. ELISA titers were expressed as the reciprocal of the highest dilution of antiserum giving an optical density (OD) at 450 nm of >0.2.

Antigen ELISA

An antigen detection ELISA was developed using the rabbit hyperimmune sera to four recombinant capsid proteins (r645, r809, r754, and r10–25), and three previously characterized VLPs, Seto 124 VLPs (rSeto) [Kobayashi et al., 2000b], Chiba 407 VLPs (rChiba) [Kobayashi et al., 2000a], and Chitta 1876 VLPs (rChitta) [Kobayashi et al., 2000c]. Microtiter plates (96-well) (Maxisorp, Nunc, Denmark) were coated with 100 μl (0.5 μg of IgG/ml) of the rabbit preimmune (1:8,800 dilution) or hyperimmune sera (1:8,800–12,000 dilutions) in a coating buffer (0.05M carbonate-bicarbonate buffer, pH 9.6) overnight at 4°C. The well was washed twice with PBS containing Tween 20 (PBS-T), and then blocked with 0.5% bovine serum albumin in PBS overnight at 4°C. One-hundred microliter of a 10% stool sample was added to the well and incubated 1 hr at room temperature. After washing the well four times with PBS-T, 100 μl of peroxidase-conjugated rabbit antiserum to VLPs were added to the well and incubated for 1 hr at room temperature. The microplate was washed four times with PBS-T, and then 100 μl of substrate, tetrametyl bentijin (TMB), was added. The plate was left for 30 min at room temperature, and the reaction was stopped with 100 μl of 0.6N H_2SO_4. The OD_{450} value of the reactions at both the hyperimmune and preimmune sera was measured. The sample was considered positive when the difference between the OD_{450} values for the hyperimmune and preimmune sera was >0.15 and the ratio was >2 [Kobayashi et al., 2000c].

Detection of NoV in Stool Specimens by RT-PCR

Extraction of viral RNA from the stools and cDNA synthesis were performed as described above. A forward primer G1F1 and a reverse primer G1R1 were used to amplify the N-terminal VP1 of GI NoV, and a forward primer G2F1 and a reverse primer G2R1 were used to amplify the same region of the GII NoV as previously described [Kobayashi et al., 2000c; Kojima et al., 2002]. The reaction was carried out in 50 μl of the solution containing 1.25 U of Ex Taq polymerase (TaKaRa), 5 μl of 10 × PCR buffer (100 mM Tris-HCl, 15 mM $MgCl_2$, 500 mM KCl), 5 μl of 25 mM deoxynucleotide mixture, 0.5 μM of each primer, and 2 μl of cDNA. After an initial denaturation at 94°C for 5 min, 35 cycles of amplification were performed using the GeneAmp PCR System 9600 (PE Biosystems). The nucleotide sequence and phylogenetic analyses were performed as described above.

Phylogenetic Analysis

Nucleotide sequences of the entire VP1 capsid protein and N-terminal VP1 were aligned with Clustal X (http://www-igbmc.u-strasbg.fr/BioInfo/). The genetic distances were calculated by Kimura's two parameter method [Kimura, 1980], and a distance matrix file was created as described previously [Katayama et al., 2002]. The phylogenetic dendrogram was constructed by the neighbor-joining method [Saitou and Nei, 1987] with 1,000 times of bootstrap resampling [Feisenstein, 1985] as described previously [Katayama et al., 2002].

Genome Sequences

The GenBank accession numbers of the entire VP1 sequences of the strains used in this study are as follows: Aichi124-89 (Seto), accession no. AB031013; Alphatron, AF195847; Amsterdam, AF195848; Appalachicola, AF414406; Arg320, AF190817; Auckland, U46039; M7, AY130761; Birmingham, AJ277612; Boxer, AF538679; Bristol, X76716; BS5, AF093797; Burwash Landing, AF414425; Camberwell, AF145896; Chiba, AB022679; Chitta, AB032758; Desert Shield, U04469; Dijon, AF472623; Erfurt, AF427118; Florida, AF414407; Girlington, AJ277606; Grimsby, AJ004864; Gwynedd, AF414408; Hawaii, U07611; Hillingdon, AJ277607; Honolulu, AF414403; Hesse, AF414406, IdahoFalls, AY054299; Kashiwa47, AB078334; LittleRock; AF414405; Leeds, AJ277608; Manchester, X86560; Mexico, U22498; Melksham, X81879; Miami, AF414410; Musgrove, AJ277614; NewOrleans, AF414422; Norwalk/68, M87661; QueenArms, AJ313030; SaintCloud, AF414427; SaitamaU1, AB039775; SaitamaU16, AB067539; SaitamaU25, AB067543; Saitama SzUG1; AB039774, Seacroft, AJ277620; Sindlesham, AJ277615; Snow Mountain , U70059; Southampton, L07418; Stavanger, AF145709; Toronto, U02030; Valetta, AJ277616; Virginia, AY038599; White River, AF414423; WhiteRose, AJ277610, Winchester, AJ277609; Wortley, AJ277618; Mc37, AY237415, WUG1, AB081723, Kashiwa 645, BD011871, Sanbu 809, BD011876, Ichikawa 754, BD011877, and Osaka 10-25, BD011881.

RESULTS

Characterization of Four NoV Strains

To classify genetically the four NoVs, the entire VP1 genes were amplified by RT-PCR and the nucleotide

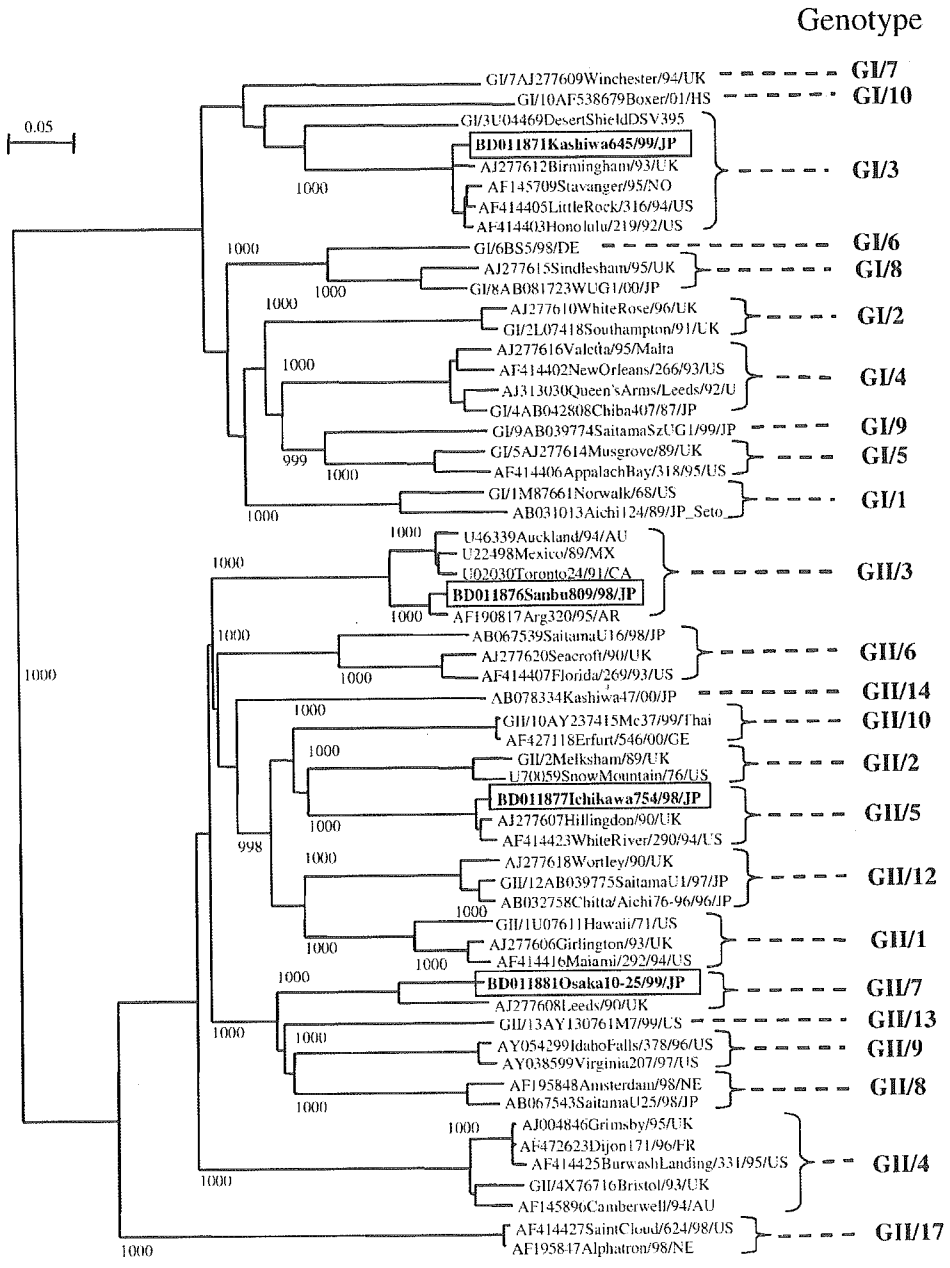

Fig. 1. Phylogenetic tree of NoVs based on entire VP1 nucleotide sequences. The numbers on each branch indicate the bootstrap values for the clusters supported by each branch. Cryptograms indicating the accession number/location or strain name/(isolate)/year/country are given for the strains. Putative genotypes are indicated for each cluster. The names GI/1 to GI/10, and GII/1 to GII/17, with the exception of GII/11, GII/15, and GII/16, are from our previous study [Katayama et al., 2002]. The complete sequences of VP1 of GII/11, GII/15, and GII/16 are not available. The four NoVs characterized in this study are shown in boldface and boxed.

sequence was determined. The phylogenetic analysis of these viruses and representative NoVs is shown in Fig. 1. Kashiwa 645 was close to Birmingham/93/UK and classified into GI/3 where Desert Shield/90/US is the representative strain. The other three strains had higher nucleotide sequence identities to GII than to the GI NoVs. Sanbu 809 was classified into GII/3 with the Toronto/93/CA and Mexico/89/MX viruses. Ichikawa 754 belongs to the GII/5 Hillingdon/90/UK genotype, whereas Osaka 10-25 was classified into GII/7 with the Leeds/90/UK virus.

Expression of the Capsid Proteins in Insect Cells

Tn5 cells (Tn5) were infected with the virus at m.o.i. 10, and the cells were incubated at 26.5°C [Li et al., 1997; Kobayashi et al., 2000a,b,c]. The expressed recombinant proteins were analyzed by 10% SDS–PAGE. A major

protein band with a molecular mass of 58–60 kDa was observed in the infected cells 2 days p.i., and the expression reached to a maximum 6 days p.i. The size of the proteins were in agreement with the molecular mass calculated from the 545, 548, 540, and 541 amino acids of Kashiwa 645, Sanbu 809, Ichikawa 754, and the Osaka 10–25 capsid proteins, respectively. The supernatant was collected at 6 days p.i., centrifuged at 100,000*g* for 2 hr in a Beckman TLA-45 rotor, and then the pellet was examined by EM. Uniform, round-shaped empty VLPs with a 38 nm diameter were observed at over 100 particles per EM field at a magnification of 20,000× (data not shown).

Antigenic Relationships of Newly Expressed Four VLPs With Previously Characterized Three VLPs

Rabbit hyperimmune antisera raised against purified r645, r809, r754, and r10–25 had titers as high as 1:409,600–1:819,200. The hyperimmune serum was not adsorbed with the wild baculovirus-infected Tn5 cell lysate, because the OD values in the antibody ELISA were negligible even when 0.5 μg protein/ml of the lysate was used to coat the microplate wells (data not shown).

The antigenic relationship of the four NoV strains was examined with three previously characterized VLPs (Table II). The highest antibody titers were detected in hyperimmune sera against homologous recombinant capsid antigens for all seven strains. Although variable cross-reactivity was detected among different recombinant antigens, higher cross-reactivity was observed with the intra-genogroup strains than with the inter-genogroup strains. For example, GI Kashiwa 645 is genetically closer to two GI NoVs, Seto 124, and Chiba 407, than the other four GII NoVs. The anti-r645 hyperimmune serum had higher antibody titers to rSeto and rChiba than to the other four GII VLPs. The hyperimmune sera to rSeto and rChiba also had higher antibody titers to the other two GI VLPs than to the other four GII VLPs. Conversely, the four GII NoVs were genetically closer to each other than to the three GI NoVs, and each GII hyperimmune serum had a higher antibody titer to the other three GII VLPs. Thus, NoVs in the same genogroup were not only genetically but also antigenically closer to one another than to those in the different genogroup.

To test further the specificity of hyperimmune serum to seven recombinant capsid proteins, an antigen ELISA was developed. In this experiment, hyperimmune sera (50 ng/well) were used to coat microplate wells to capture the recombinant VLPs. As shown in Table III, the OD values in the homologous reaction decreased in a dose-dependent manner. Little cross-reactions between different genotypes were observed. In contrast, high sensitivity was found in the homologous reactions although the limit of detection is 0.4 ng/ml as observed in the reaction with rChiba and r809, and this corresponds to 2.5×10^6 particles of NoVs.

Detection of NoV Antigen in Stool Specimens

To test the performance of the antigen ELISA, NoVs detection was carried out with stool specimens from acute gastroenteritis patients. Microplates were coated with the rabbit preimmune or hyperimmune sera to capture the antigen in the stool specimens, and peroxidase-conjugated antiserum was used as the detector antibody. In control experiments, antisera against recombinant VLPs efficiently captured at least 4 ng of the homologous antigen but not the heterologous antigen (Table III). The preimmune sera did not capture any of the VLPs at any concentration (the OD value was usually less than 0.05). Two to three representative stool specimens were selected from outbreaks associated with the GI/1, GI/3, GI/4, GII/3, GII/5, GII/7, and GII/12 genotypes to evaluate the antigen ELISA. All specimens were positive by RT-PCR targeting the N-terminal capsid region, and the amplified fragments were genotyped by sequencing analyses followed by phylogenetic analyses (Table IV). All hyperimmune sera except GI/1 Seto reacted only to the homologous genotype samples. In Seto virus detection, all three GI/3 and one of the three GI/4 samples were positive by ELISA. Interestingly, stool samples 98-MC4 (GI/1) and 2000K-518 (GI/3) were negative by EM but positive by the ELISA, suggesting that the antigen ELISA established in this study is capable of detecting disrupted NoV

TABLE II. ELISA Titers of Seven Hyperimmune Antisera Against VLPs

VLPs[a]		Hyperimmune sera against VLP antigens						
		GI/1 Seto	GI/3 645	GI/4 Chiba	GII/3 809	GII/5 754	GII/7 10–25	GII/12 Chitta
GI/1	rSeto	**819200**[b]	25600	12800	200	12800	1600	3200
GI/3	r645	102400	**819200**	25600	400	12800	6400	6400
GI/4	rChiba	102400	25600	**819200**	800	6400	6400	6400
GII/3	r809	25600	6400	6400	**819200**	51200	51200	25600
GII/5	r754	25600	6400	3200	25600	**819200**	25600	51200
GII/7	r10-25	12800	12800	6400	25600	51200	**819200**	25600
GII/12	rChitta	25600	1600	1600	25600	51200	25600	**409600**

[a]Four VLPs: r645, r809, r754, and r10-25 and their hyperimmune sera were prepared in this study, and three VLPs: rSeto, rChiba, and rChitta and their hyperimmune sera were prepared in our previous studies[Kobayashi et al., 2000a,b,c].
[b]ELISA titers were expressed as the reciprocal of the highest dilution of antiserum giving an optical density (OD) at 450 nm of >0.2. Homologous titers are shown in boldface.